DTU

Christian Berggreen

Aakash Moncy

Investigating the Growth of Matrix Cracks under Biaxial Strain Control Fatigue using Cruciform Specimens

(Full version – reduced version will be presented at the conference)

31 July – 4 August 2023

Contents

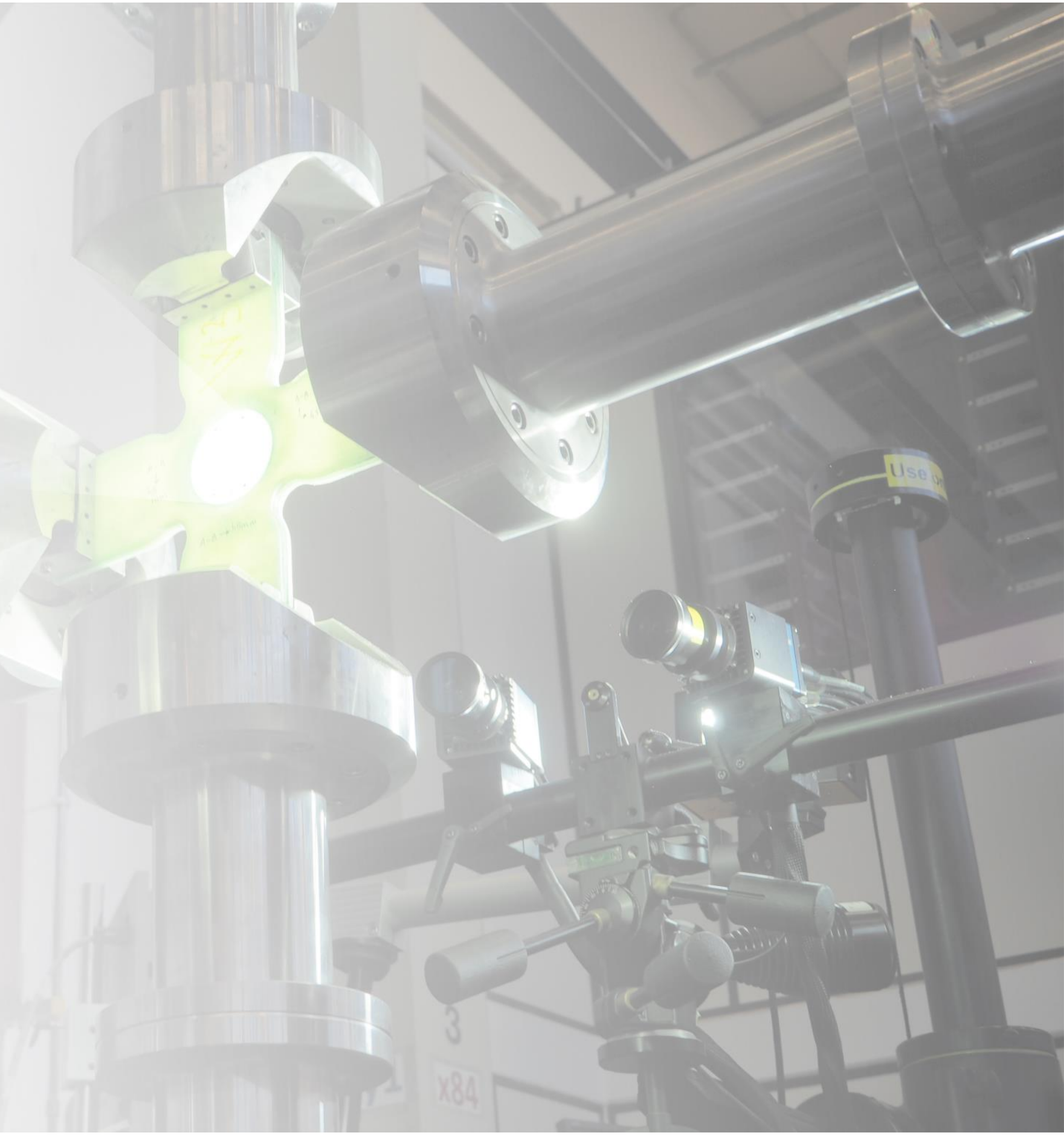

1

Introduction

Introduction

Overview of length-scales

A MULTI-SCALE TESTING AND MODELLING FRAMEWORK

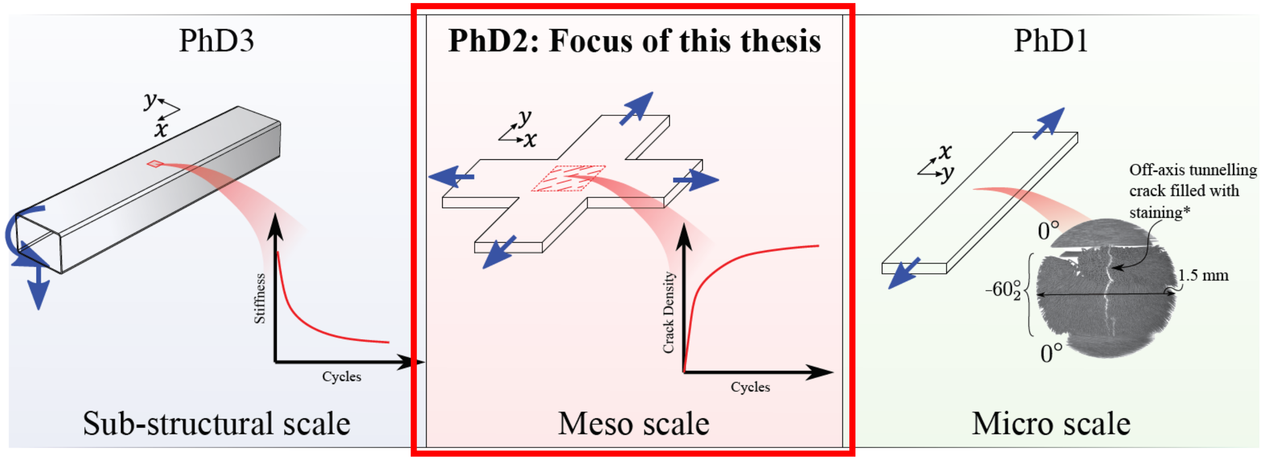

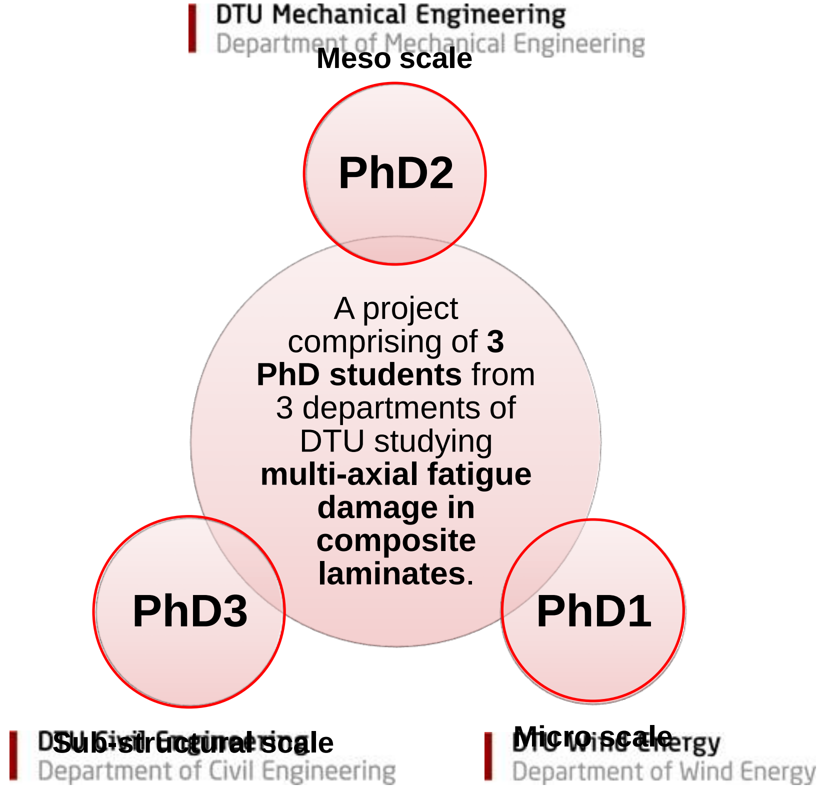

Introduction

Overview of the damage mechanisms

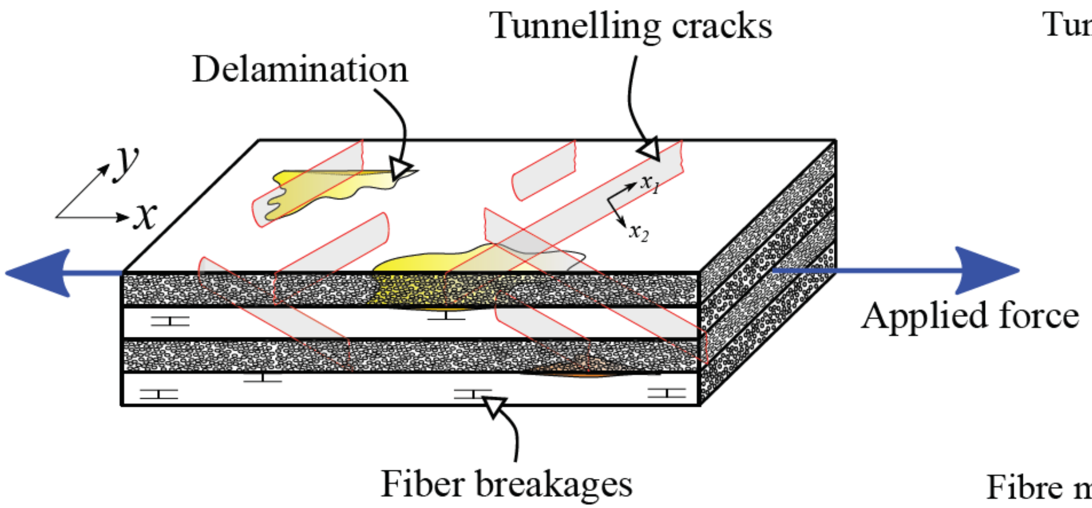

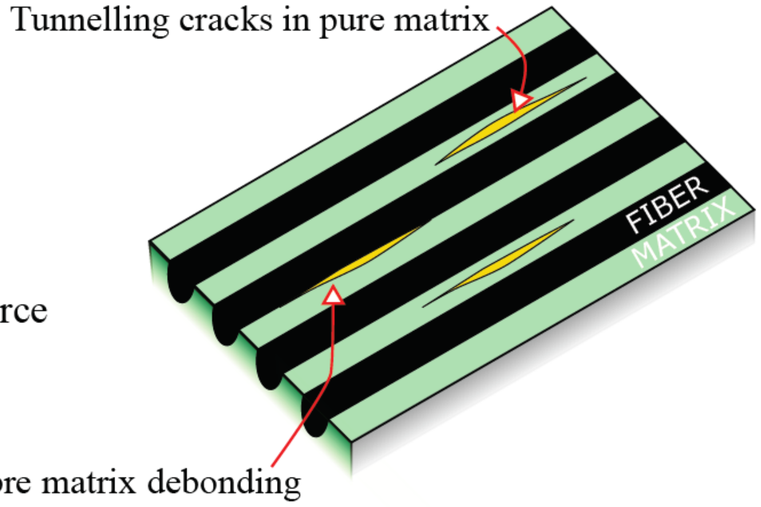

Fatigue in composite laminates is quite complex, primarily due to the damage process being **multi-scale** in nature.

Damage mechanisms is highly dependent on the layup sequence.

The damage progression of a typical multi-directional composite laminates includes -

Tunnelling cracks in off-axis layers
+
Isolated fibre breakages

Saturation of tunneling cracks

Multiple delaminations
+
Fibre fractures

Failure of the laminate

Introduction

Overview of the damage mechanisms

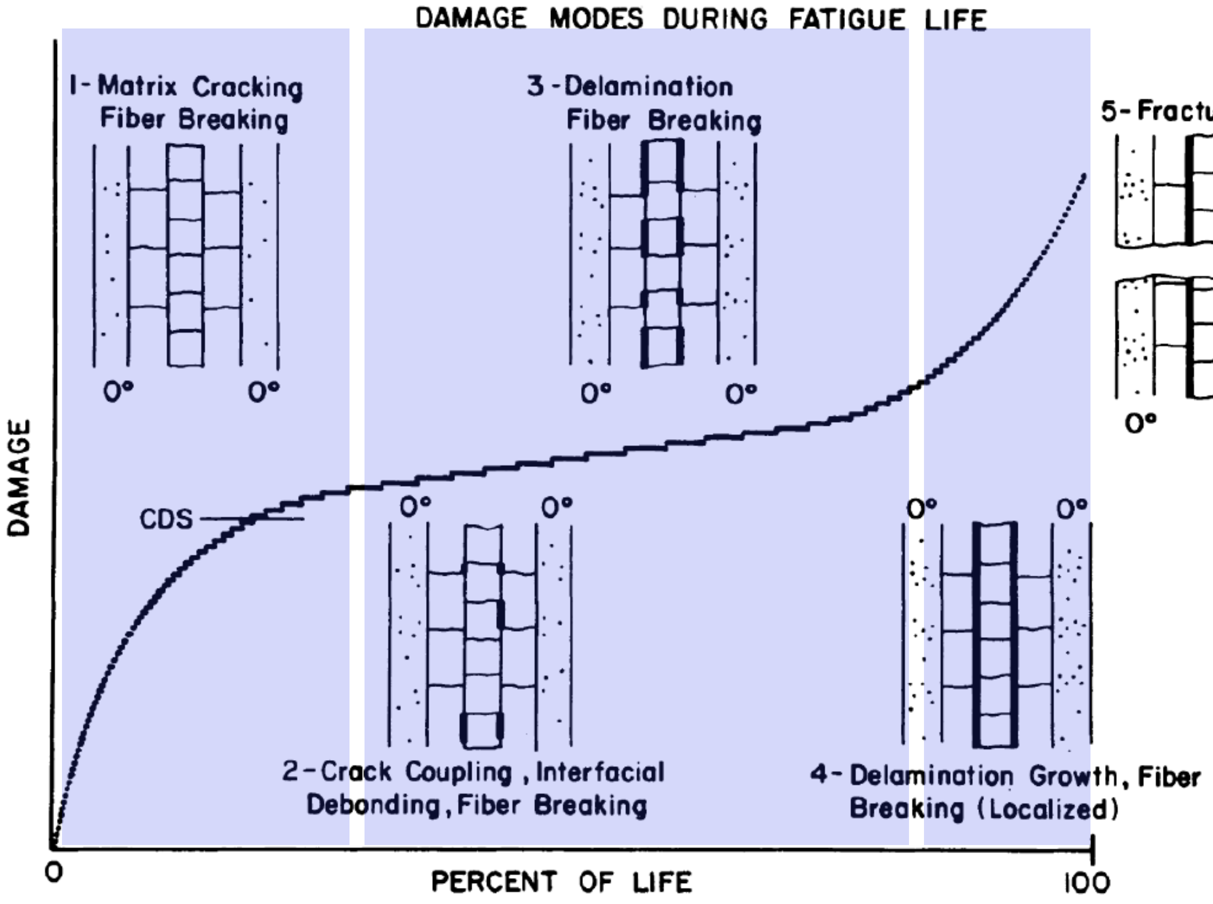

K.L Reifsneider. “Fatigue of composite materials”. In: vol. 4. Elsevier, 1991, pp. 1–519. ISBN: 978-0-444-70507-5.

The different damage modes are often interacting with each other.

Damage behaviour in composite laminates is highly non-linearly, making prediction of damage not a simple task.

Fatigue damage in non-crimp fabric composites are even more complicated due to the use of backing bundles.

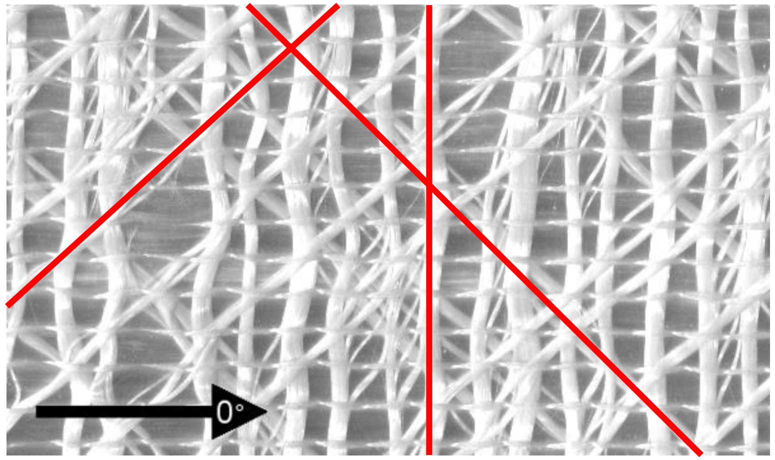

Introduction

Tunnelling cracks

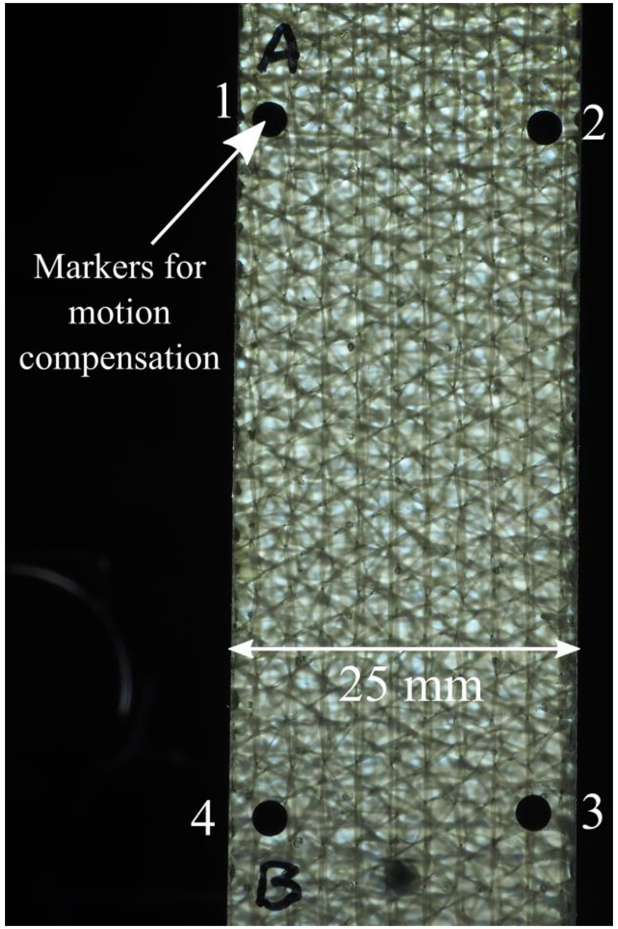

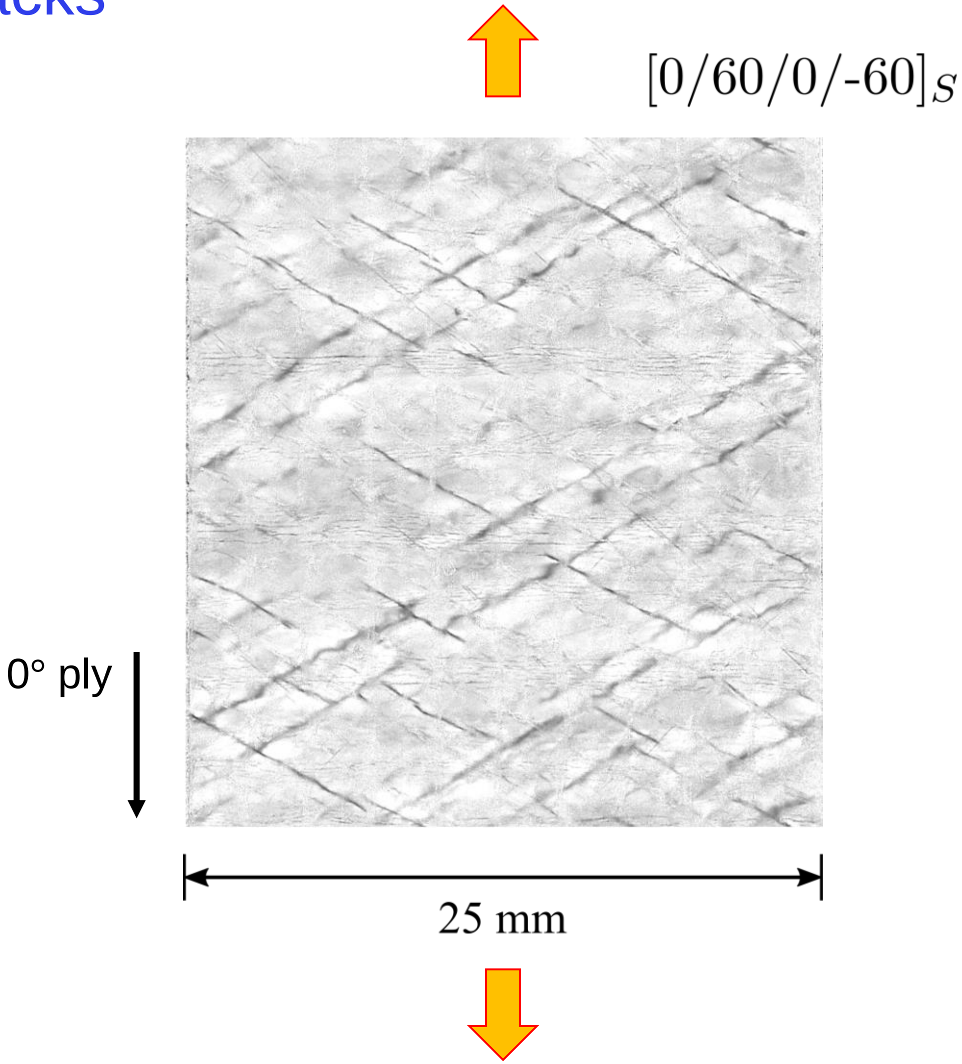

Not all cracks appear at the same time.

Damage is progressive in nature.

Crack fronts can be interacting or non-interacting.

The **global** average crack density is calculating using –

$$\rho = \frac{\sum_{i=1}^{n} L_i}{A}$$

J.A. Glud et al. “Automated counting of off-axis tunnelling cracks using digital image processing”. In: Composites Science and Technology 125 (2016), pp. 80–89.

Introduction

Predicting tunneling cracks

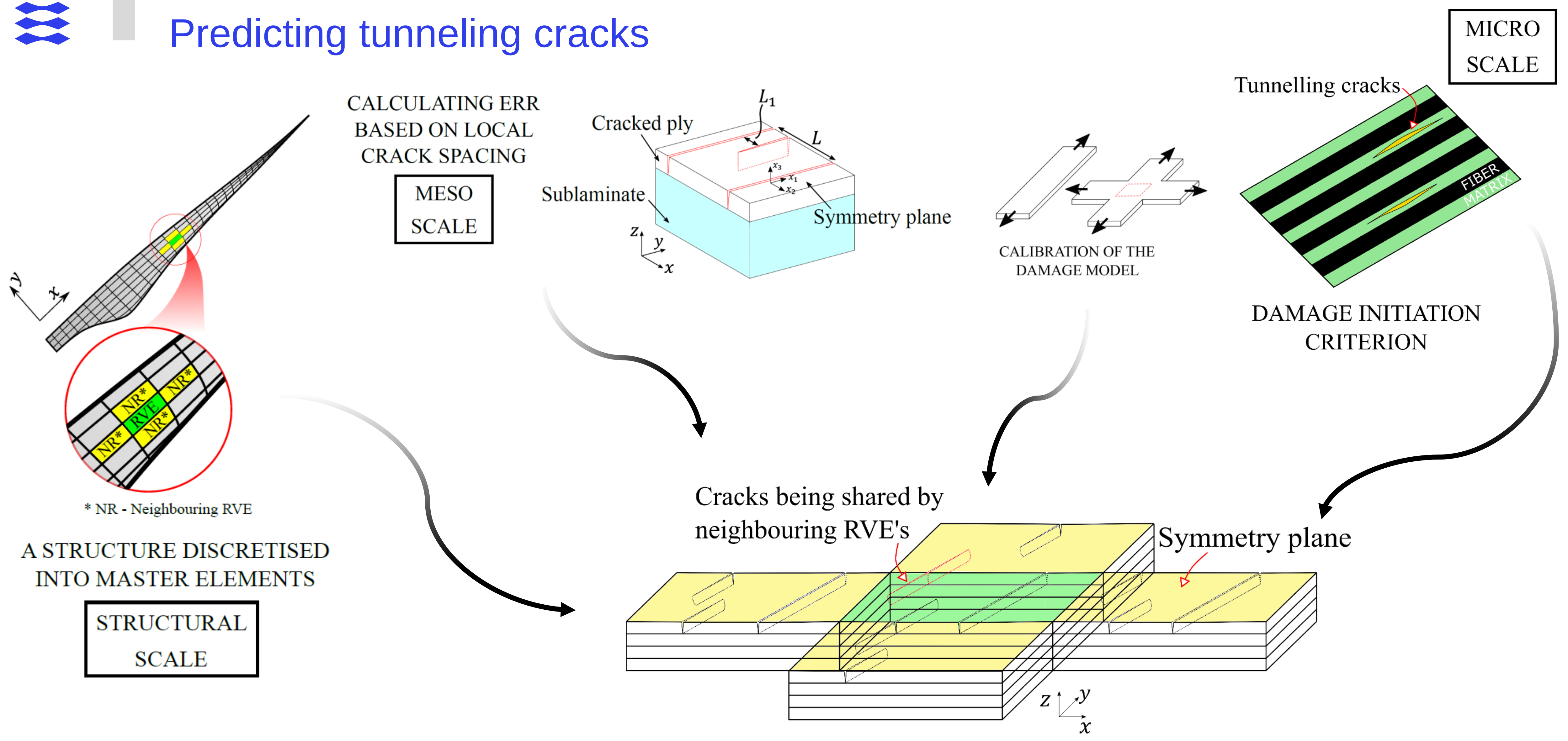

Introduction

Predicting tunneling cracks

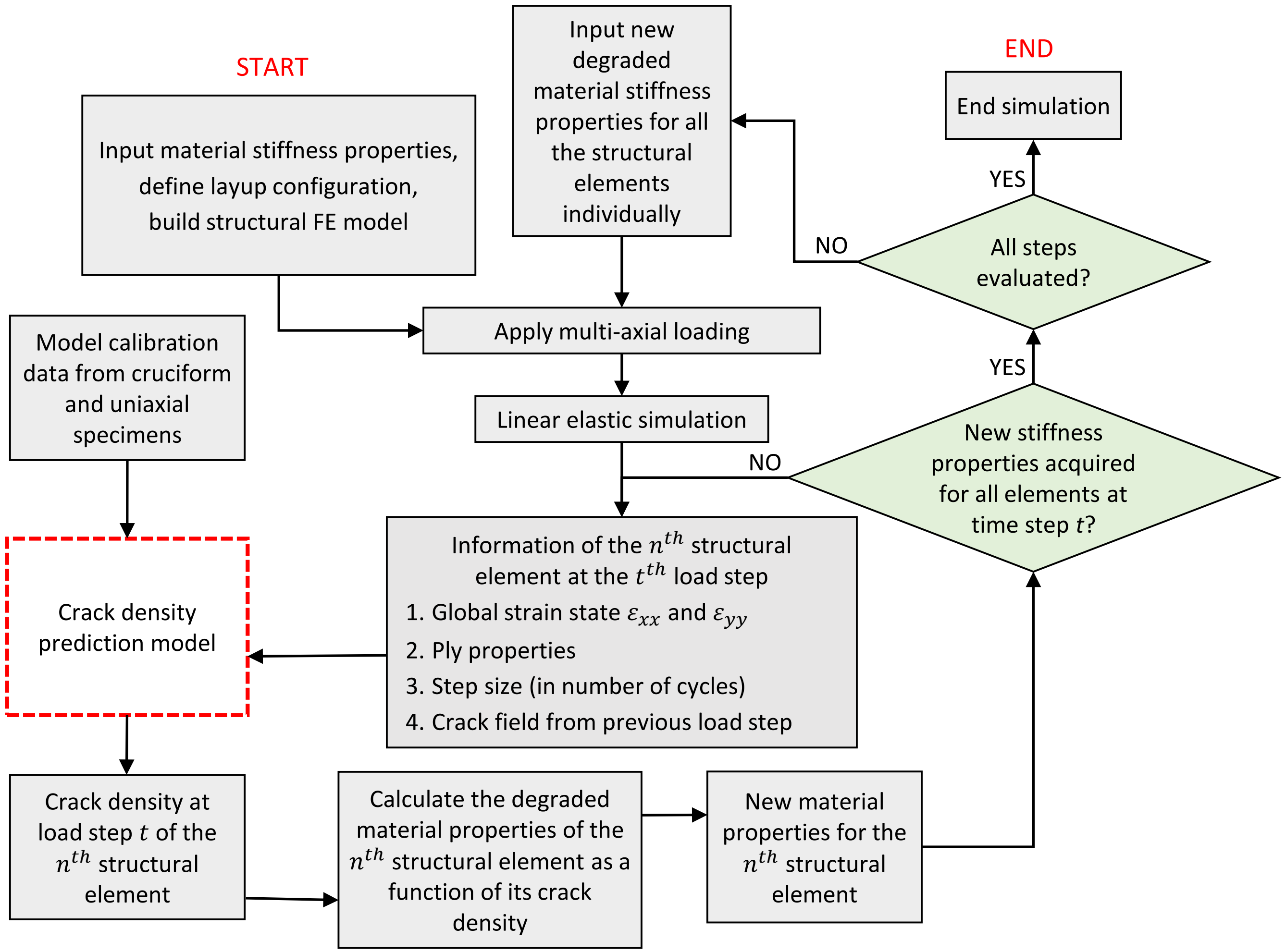

2

Cruciform specimens and anisotropy

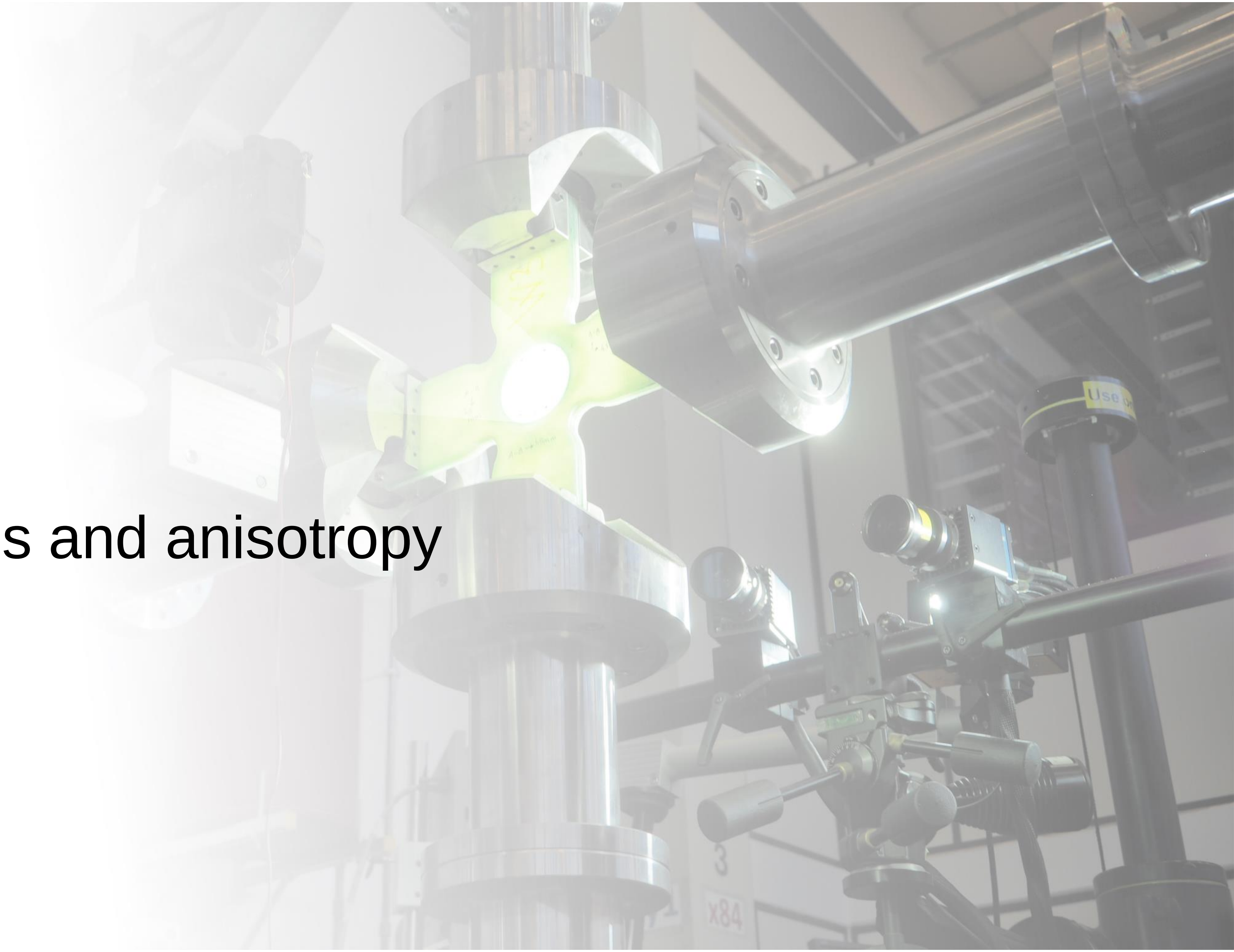

Cruciform specimens and anisotropy

Influence of material anisotropy

$$\theta = 20°,\ 40°,\ 60° \text{ and } 80°$$

<u>Average</u> weighted standard deviation for the ply level stresses

$$\xi_{avg} = (\xi_{11} + \xi_{22} + \xi_{12})/3$$

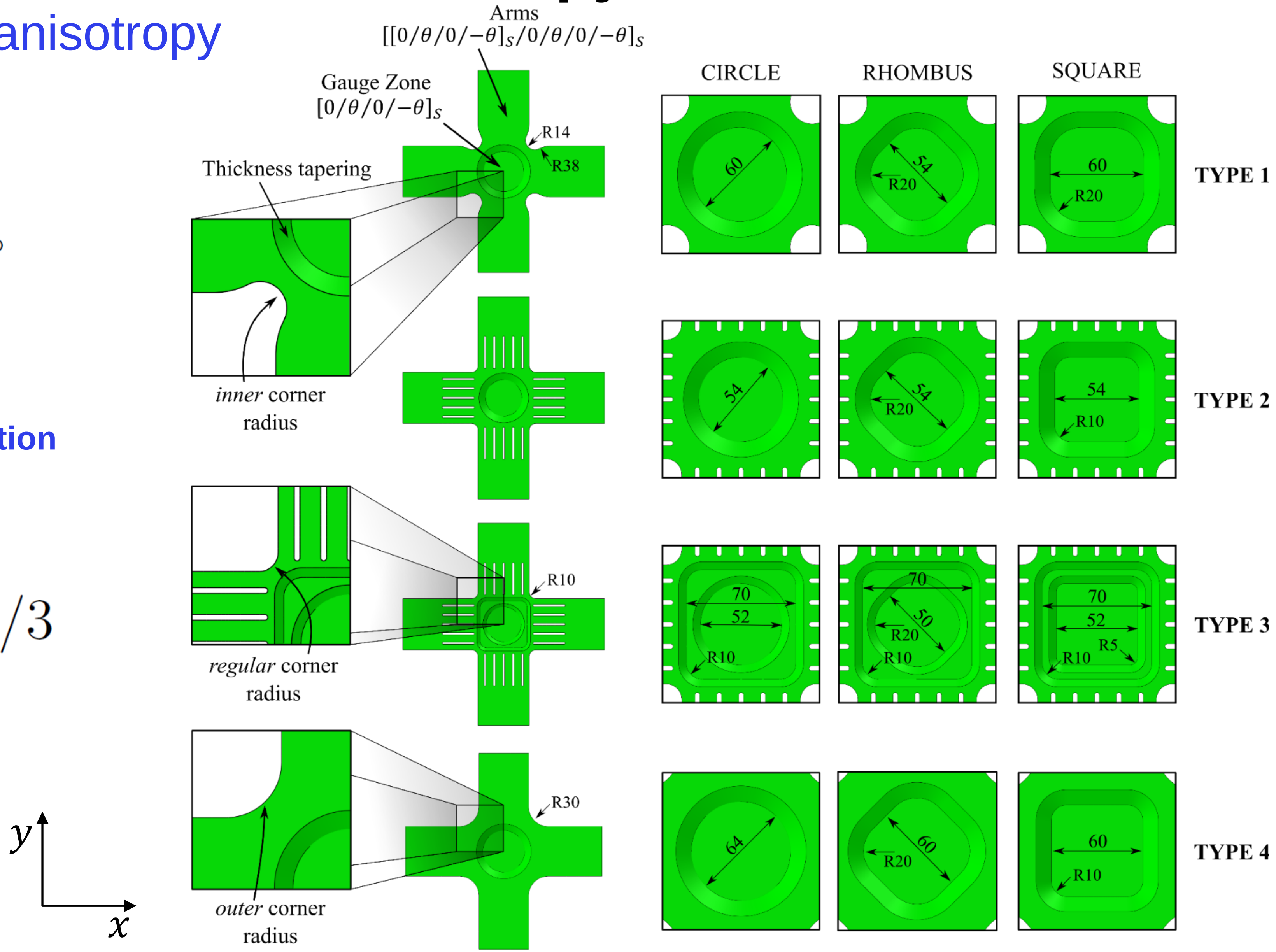

Cruciform specimens and anisotropy

Influence of material anisotropy

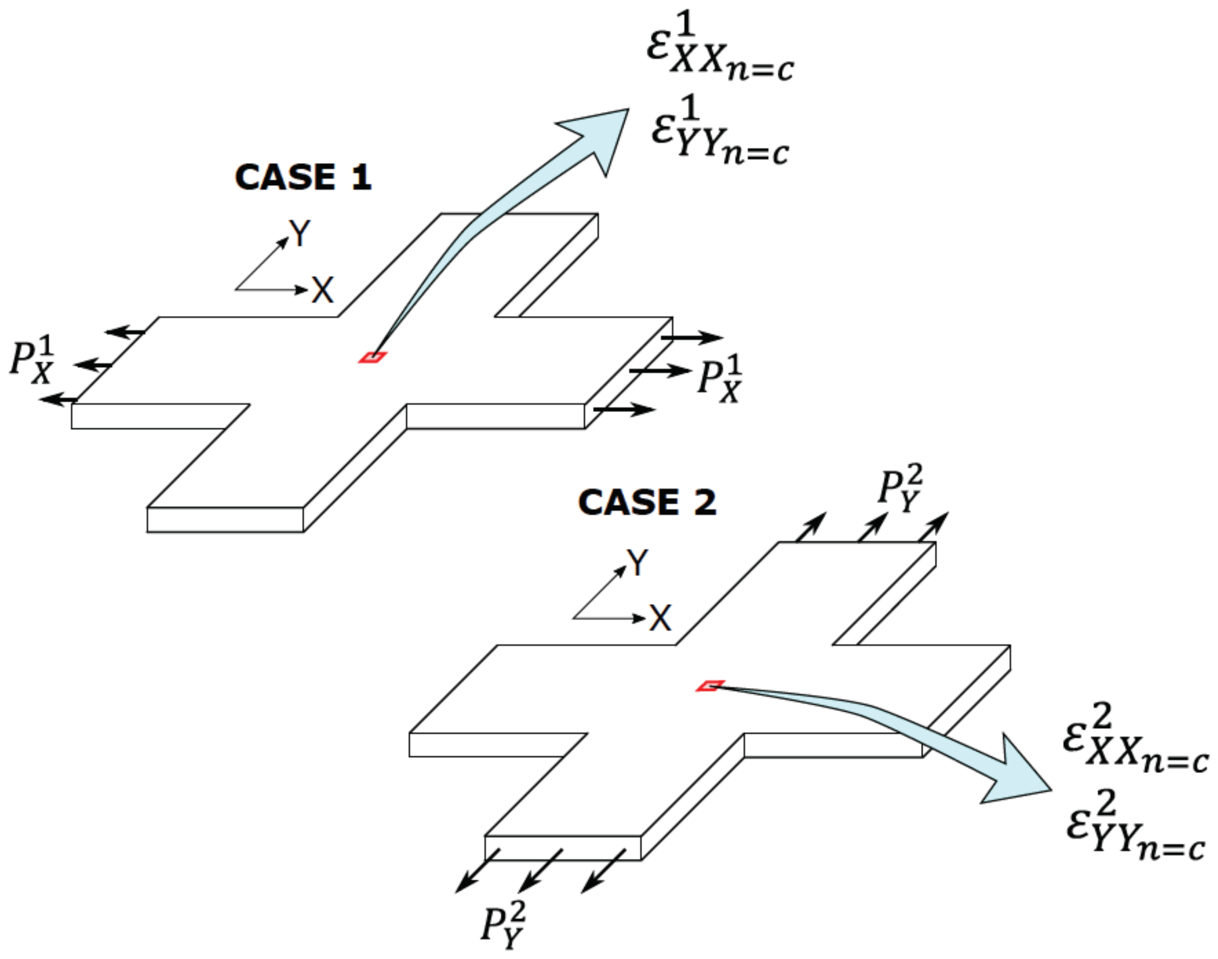

Stress state under any loading condition

$$\sigma_{ij_n} = k_1 \cdot \sigma^1_{ij_n} + k_2 \cdot \sigma^2_{ij_n}$$

$$k_1 = \frac{-\varepsilon^R_{XX_c} \cdot \varepsilon^2_{YY_c} + \varepsilon^R_{YY_c} \cdot \varepsilon^2_{XX_c}}{\varepsilon^2_{XX_c} \cdot \varepsilon^1_{YY_c} - \varepsilon^2_{YY_c} \cdot \varepsilon^1_{XX_c}}$$

$$k_2 = \frac{\varepsilon^R_{XX_c} \cdot \varepsilon^1_{YY_c} - \varepsilon^R_{YY_c} \cdot \varepsilon^1_{XX_c}}{\varepsilon^2_{XX_c} \cdot \varepsilon^1_{YY_c} - \varepsilon^2_{YY_c} \cdot \varepsilon^1_{XX_c}}$$

2 Cruciform specimens and anisotropy

Influence of material anisotropy

Layup 1
$[0/20/0/-20]_S$

Layup 2
$[0/40/0/-40]_S$

Layup 3
$[0/60/0/-60]_S$

Layup 4
$[0/80/0/-80]_S$

Performance of the best and worst cruciform geometries, with changing anisotropy level.

2 Cruciform specimens and anisotropy

Conclusions

- A single cruciform specimen cannot be used for all biaxial load ratios or layup configurations.
- The anisotropy of composite materials is seen as one of the biggest challenges in standardizing the cruciform specimen.
- Cruciform specimens with a rhombus gauge zone shape performed better than a circular or a squared gauge zone shape.
- Future work should involve optimization of the specimen for avoiding the usage of different specimen designs for different biaxial load ratio.

3

Biaxial cyclic tests using cruciform specimens

Biaxial cyclic tests using cruciform specimens

The biaxial testing machine

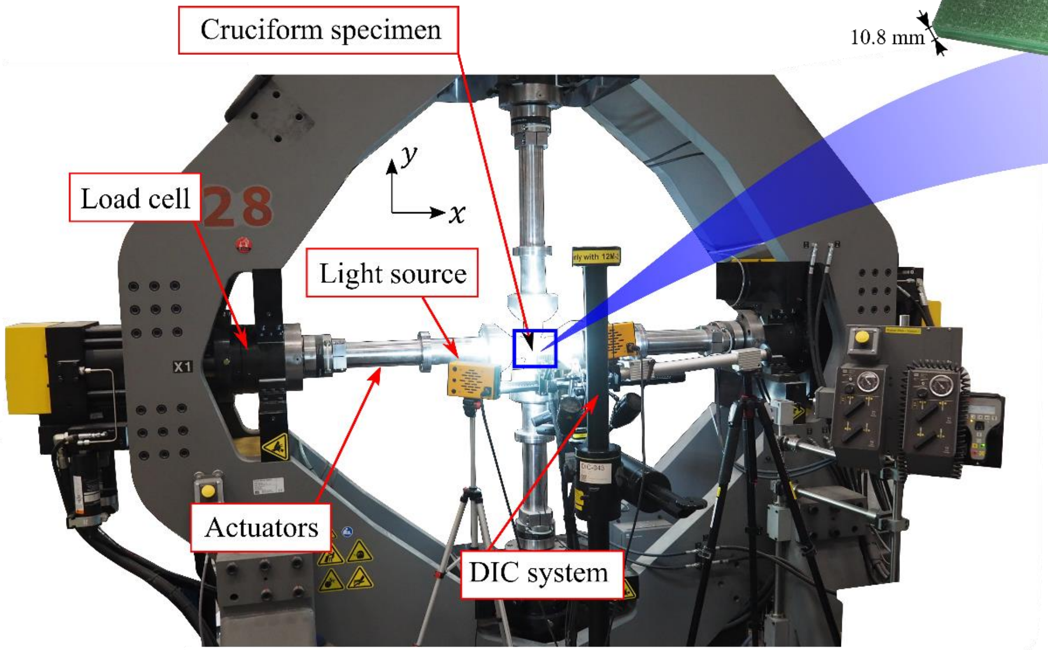

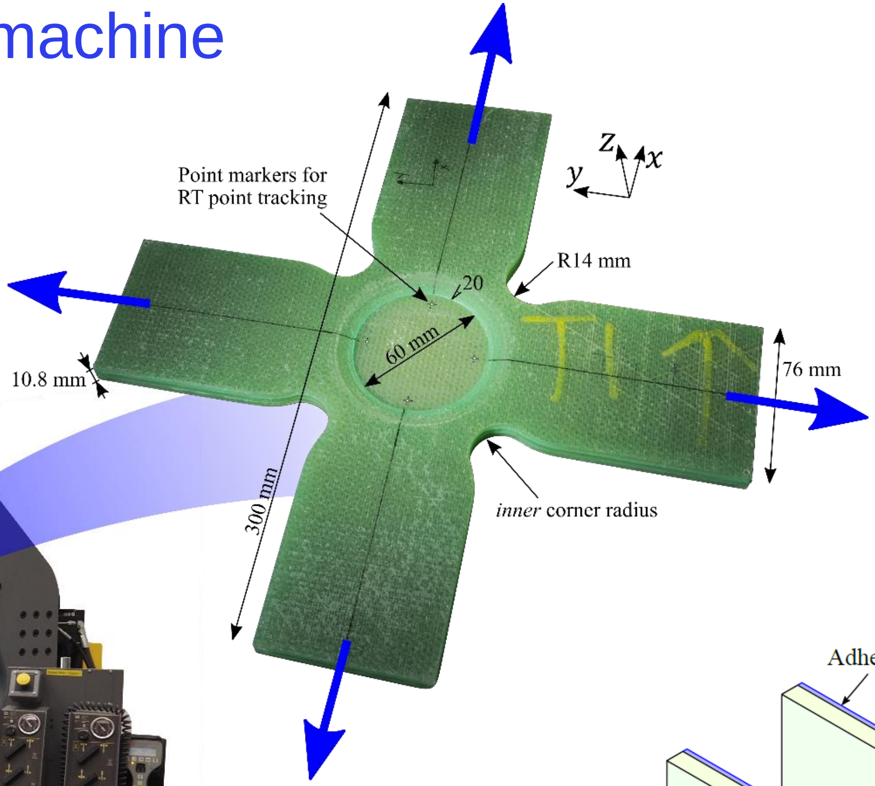

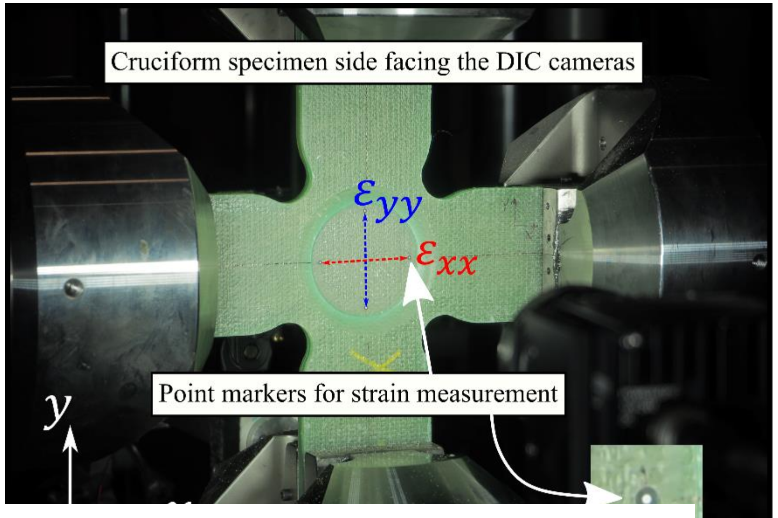

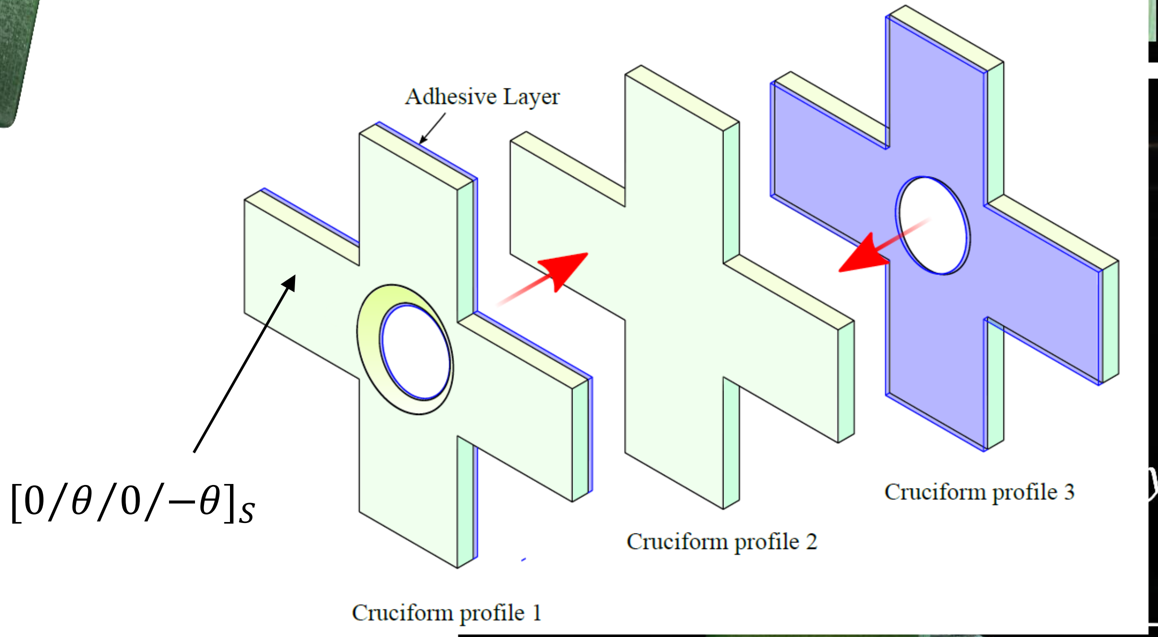

Biaxial cyclic tests using cruciform specimens

Passive strain control method

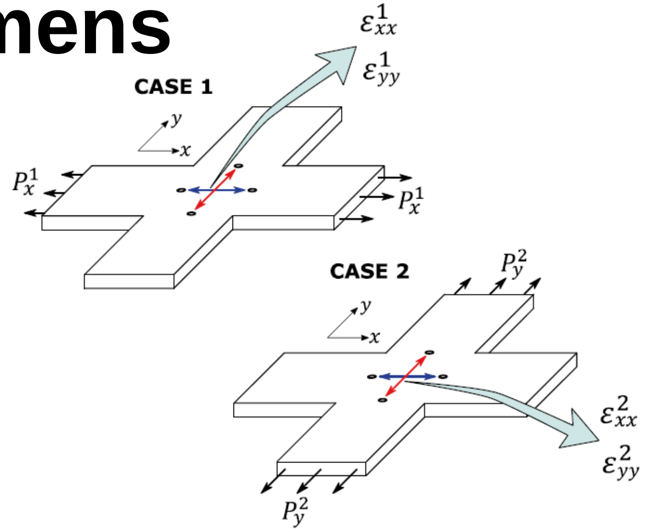

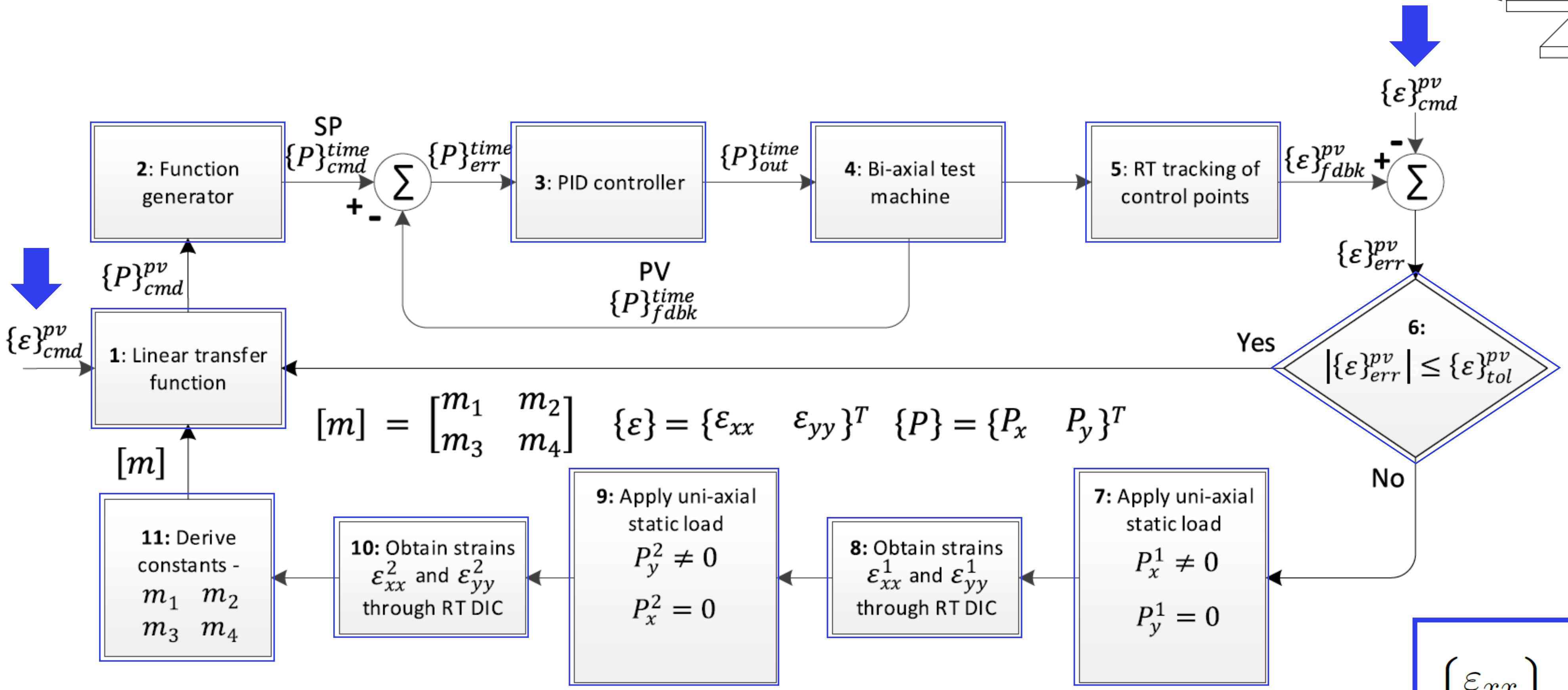

$$\begin{Bmatrix} \varepsilon_{xx} \\ \varepsilon_{yy} \end{Bmatrix} = \begin{bmatrix} m_1 & m_2 \\ m_3 & m_4 \end{bmatrix} \begin{Bmatrix} P_x \\ P_y \end{Bmatrix}$$

Biaxial cyclic tests using cruciform specimens

Active strain control method

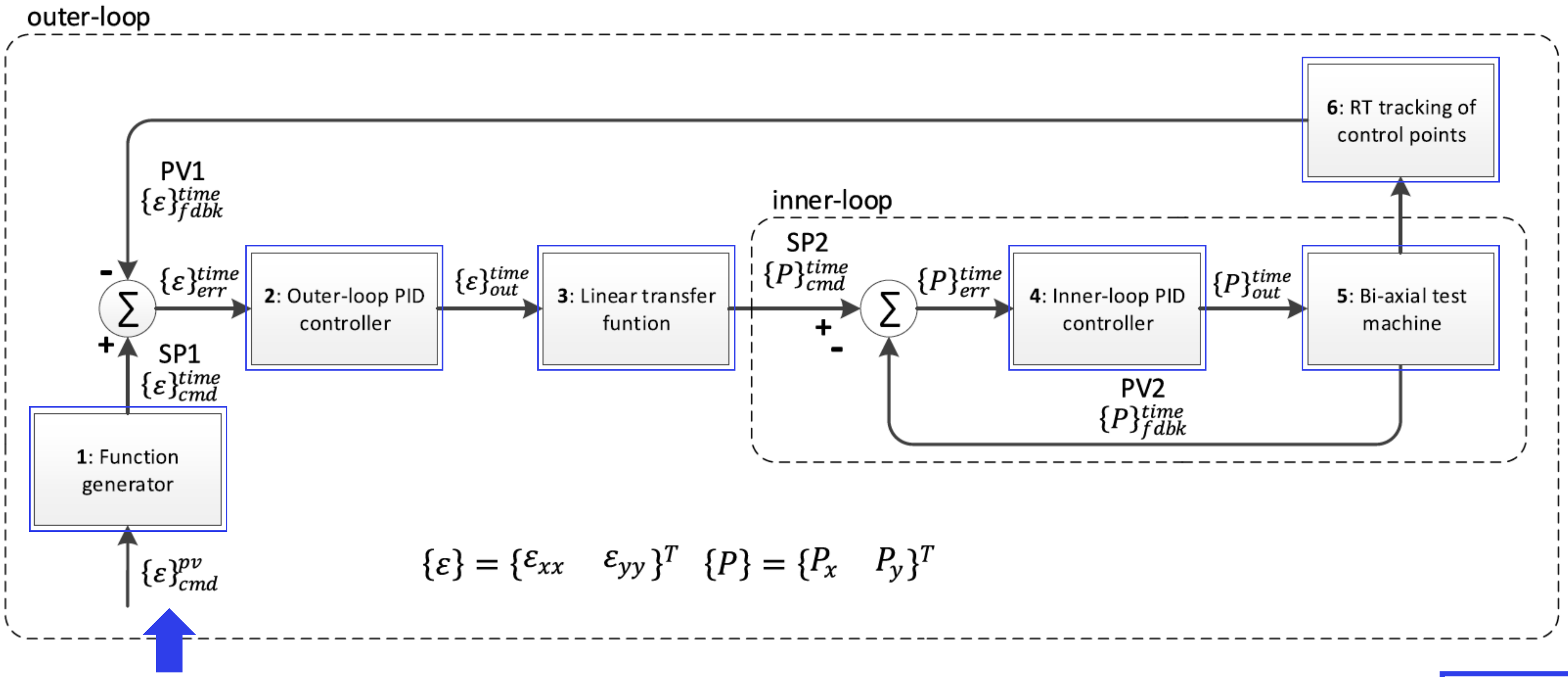

$$\begin{Bmatrix} \varepsilon_{xx} \\ \varepsilon_{yy} \end{Bmatrix} = \begin{bmatrix} m_1 & m_2 \\ m_3 & m_4 \end{bmatrix} \begin{Bmatrix} P_x \\ P_y \end{Bmatrix}$$

Biaxial cyclic tests using cruciform specimens

Comparison between the active and passive strain control methods

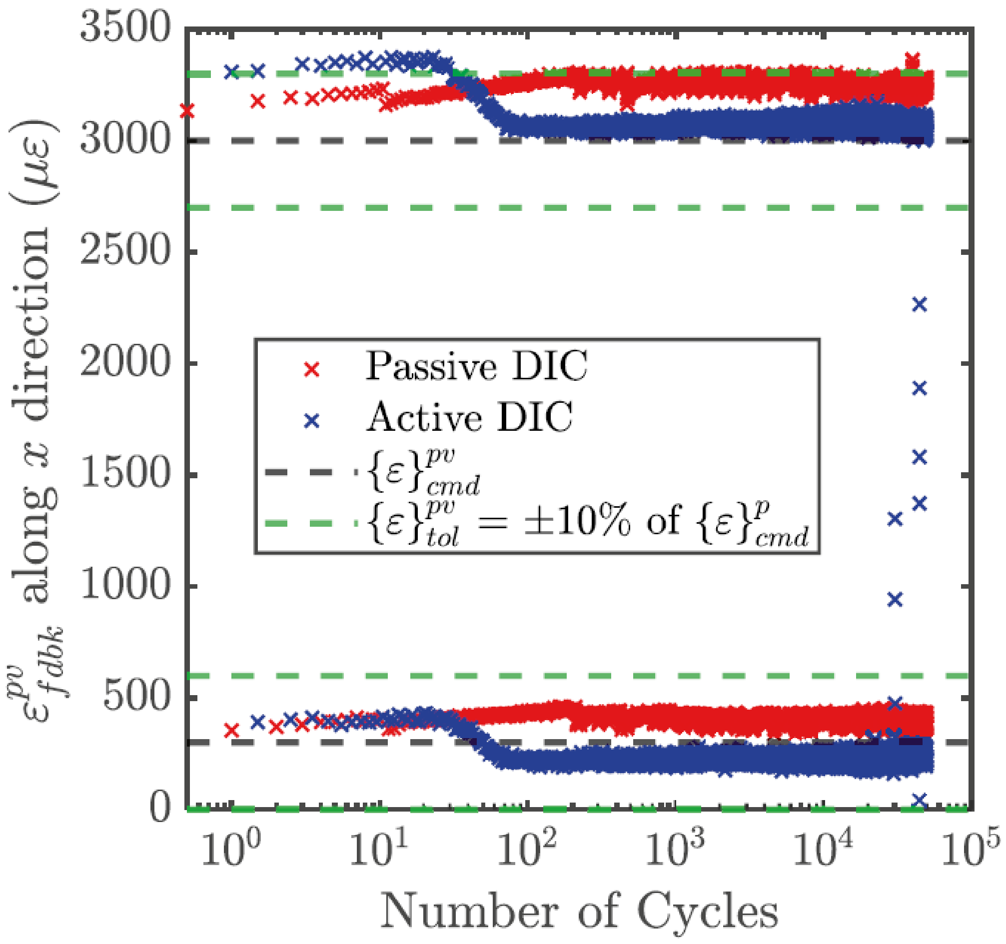

3 Biaxial cyclic tests using cruciform specimens

Comparison between the active and passive strain control methods

Active	Passive
T1: $\{\varepsilon\}^p_{cmd} = \{2000\ 2000\}^T \mu\varepsilon$	T1: $\{\varepsilon\}^p_{cmd} = \{2000\ 2000\}^T \mu\varepsilon$
T2: $\{\varepsilon\}^p_{cmd} = \{3000\ 3000\}^T \mu\varepsilon$	T2: $\{\varepsilon\}^p_{cmd} = \{3000\ 3000\}^T \mu\varepsilon$
T5: $\{\varepsilon\}^p_{cmd} = \{4000\ 4000\}^T \mu\varepsilon$	T5: $\{\varepsilon\}^p_{cmd} = \{4000\ 4000\}^T \mu\varepsilon$
T6: $\{\varepsilon\}^p_{cmd} = \{4000\ -2584\}^T \mu\varepsilon$	T6: $\{\varepsilon\}^p_{cmd} = \{4000\ -2584\}^T \mu\varepsilon$
T8: $\{\varepsilon\}^p_{cmd} = \{4500\ -2907\}^T \mu\varepsilon$	T8: $\{\varepsilon\}^p_{cmd} = \{4500\ -2907\}^T \mu\varepsilon$
T9: $\{\varepsilon\}^p_{cmd} = \{5000\ -3230\}^T \mu\varepsilon$	T9: $\{\varepsilon\}^p_{cmd} = \{5000\ -3230\}^T \mu\varepsilon$
T3: $\{\varepsilon\}^p_{cmd} = \{3000\ 1500\}^T \mu\varepsilon$	T3: $\{\varepsilon\}^p_{cmd} = \{3000\ 1500\}^T \mu\varepsilon$
T4: $\{\varepsilon\}^p_{cmd} = \{3500\ 1750\}^T \mu\varepsilon$	T4: $\{\varepsilon\}^p_{cmd} = \{3500\ 1750\}^T \mu\varepsilon$
T7: $\{\varepsilon\}^p_{cmd} = \{4000\ 2000\}^T \mu\varepsilon$	T7: $\{\varepsilon\}^p_{cmd} = \{4000\ 2000\}^T \mu\varepsilon$

- γ is the ratio of average $\{\varepsilon\}^k_{fdbk}$ and $\{\varepsilon\}^k_{cmd}$
- Ideal value of γ should be 1.
- CoV is the coefficient of variance in $\{\varepsilon\}^k_{fdbk}$.
- $k = p$ or v depending on whether the peak of the valley strain of the sinusoidal loading is evaluated.

3 Biaxial cyclic tests using cruciform specimens

Conclusions

- The cascade architecture (Active strain-control), was found to perform better than the conditional algorithm (passive strain-control).
- The active strain-control can have difficulties in maintaining the desired strain state under very large stiffness degradation.
- It risks system instability due to temporary loss of track of the point markers.
- A hybrid active-passive control method is proposed as a future work that provides the accuracy of the cascade architecture and the flexibility of recalculating the coupling matrix through the conditional algorithm.

4

Growth of tunnelling cracks under strain-control

4 Growth of tunnelling cracks under strain-control

Multiplication of tunneling cracks

Interacting crack front

Non-interacting crack front

Growth of tunnelling cracks under strain-control

Multiplication of tunneling cracks

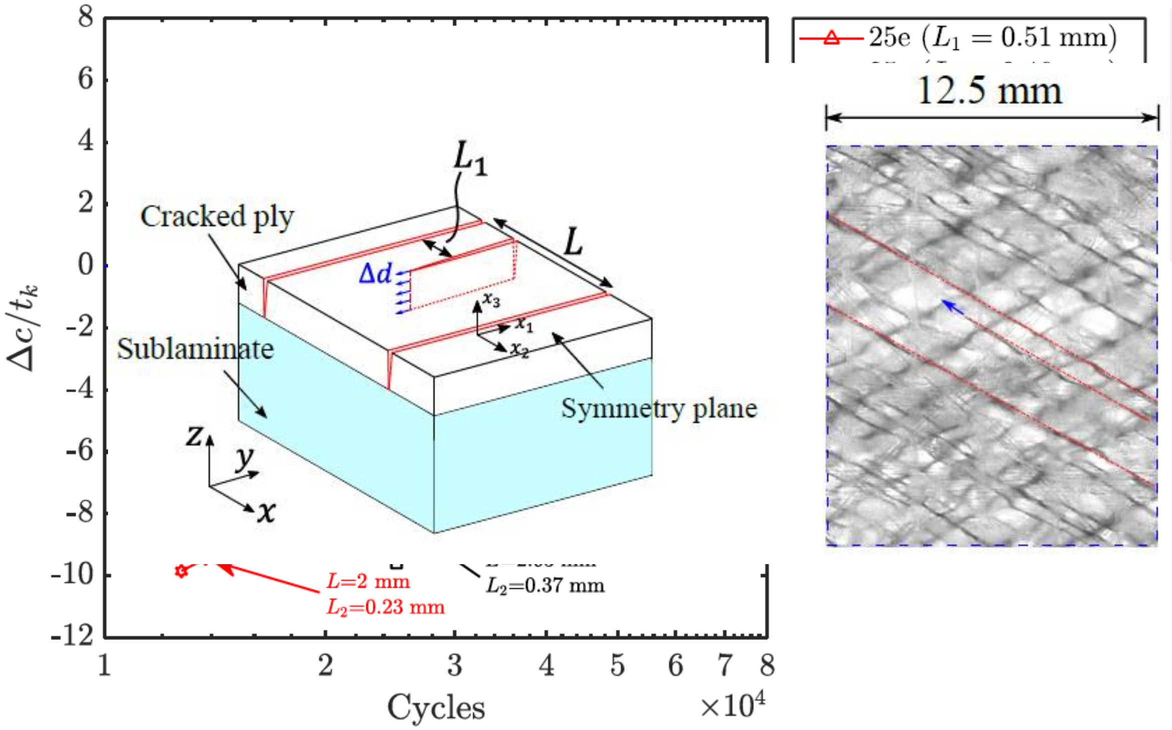

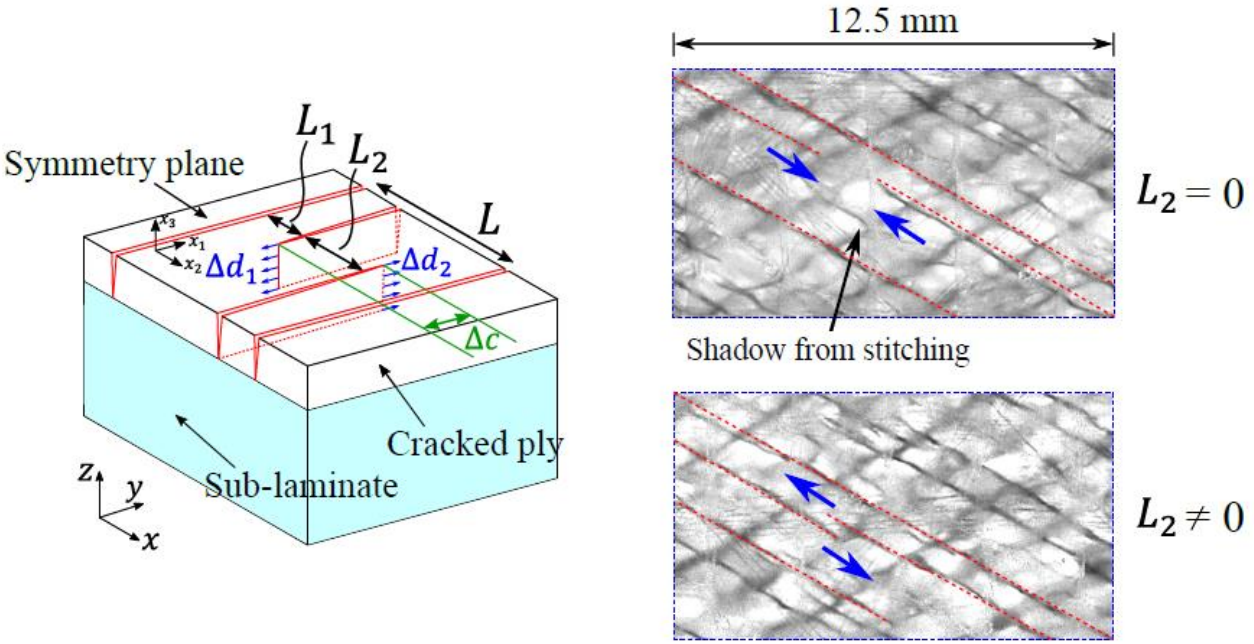

4 Growth of tunnelling cracks under strain-control

Growth of non-interacting cracks

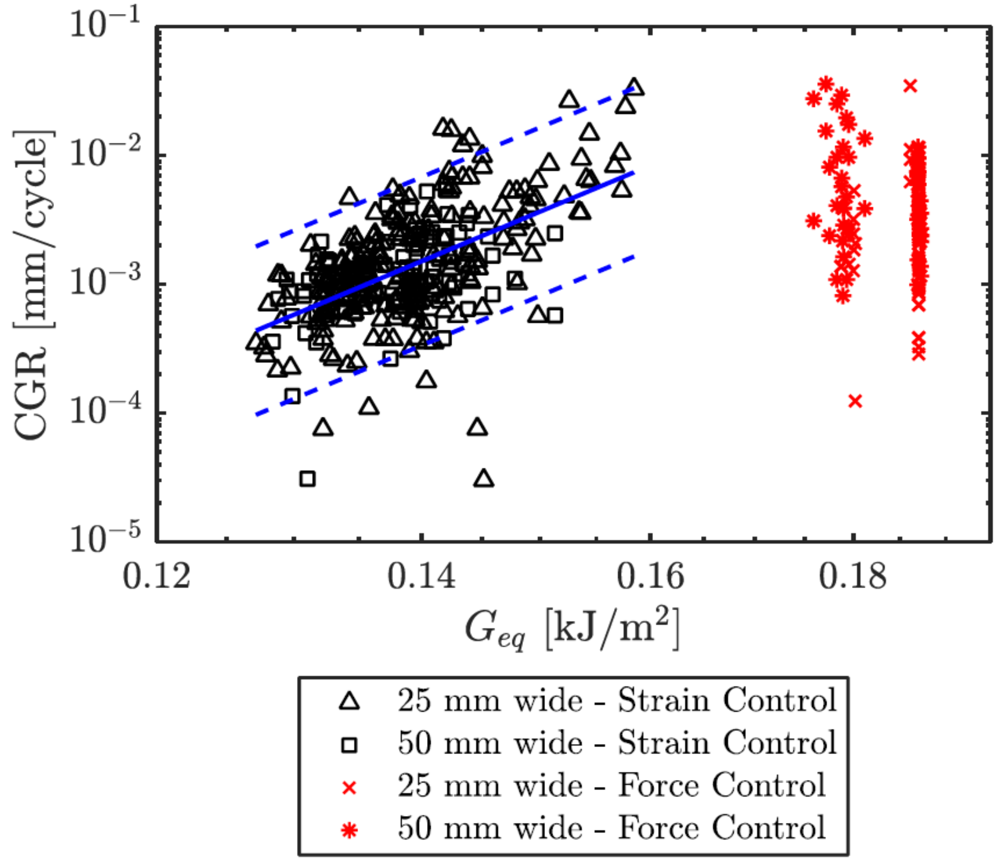

$$G_{ss} = \underbrace{\boxed{\frac{1}{2t_k}\int_0^{t_k}\sigma_{220}^k(z)\delta_2^{k0}(z)dz}}_{G_I} + \underbrace{\boxed{\frac{1}{2t_k}\int_0^{t_k}\tau_{120}^k(z)\delta_1^{k0}(z)dz}}_{G_{II}}$$

$$G_{eq} = G_I \text{ for MM} \leq \text{MM}^* \qquad \text{MM} = \frac{G_{II}}{G_I + G_{II}}$$

$$G_{eq} = (\sqrt{1-\text{MM}} + \sqrt{\text{MM}})^2(G_I + G_{II}) \text{ for MM} \geq \text{MM}^*$$

J. Glud, P. Carraro, M. Quaresimin, J. Dulieu-Barton, O. Thomsen and L. Overgaard, *A damage based model for mixed-mode crack propagation in composite laminates*, Composites Part A, vol. 107, pp. 421-431, 2018

4 Growth of tunnelling cracks under strain-control

Growth of non-interacting cracks

4 Growth of tunnelling cracks under strain-control

Growth of interacting cracks

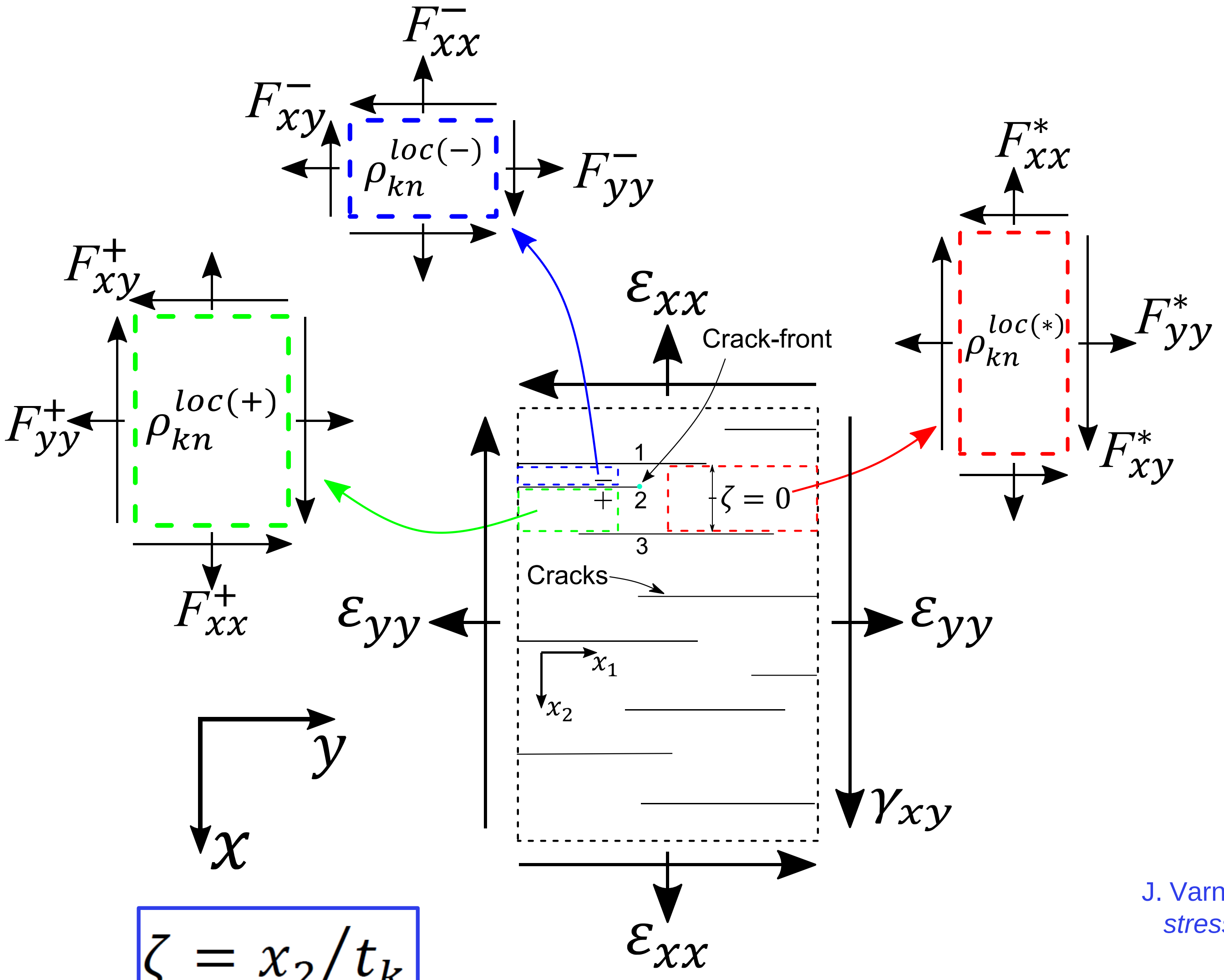

$$\boxed{\zeta = x_2/t_k}$$

$$G_{ss} = \underbrace{\boxed{\frac{1}{2}\sigma_{22}^{k}\left(\rho_{kn}^{loc(*)},\zeta\right)\tilde{\delta}_{2an}^{k}\left(\rho_{kn}^{loc(-)},\rho_{kn}^{loc(+)}\right)}}_{G_I} + \underbrace{\boxed{\frac{1}{2}\tau_{12}^{k}\left(\rho_{kn}^{loc(*)},\zeta\right)\tilde{\delta}_{1an}^{k}\left(\rho_{kn}^{loc(-)},\rho_{kn}^{loc(+)}\right)}}_{G_{II}}$$

$$\rho_k^{loc} = \frac{1}{L}$$

J. Varna. *Strategies for stiffness analysis of laminates with microdamage: Combining average stress and crack face displacement based methods*. In: *Zamm Zeitschrift Fur Angewandte Mathematik Und Mechanik* 95.10 (2015), pp. 1081–1097

4 Growth of tunnelling cracks under strain-control

Growth of interacting cracks

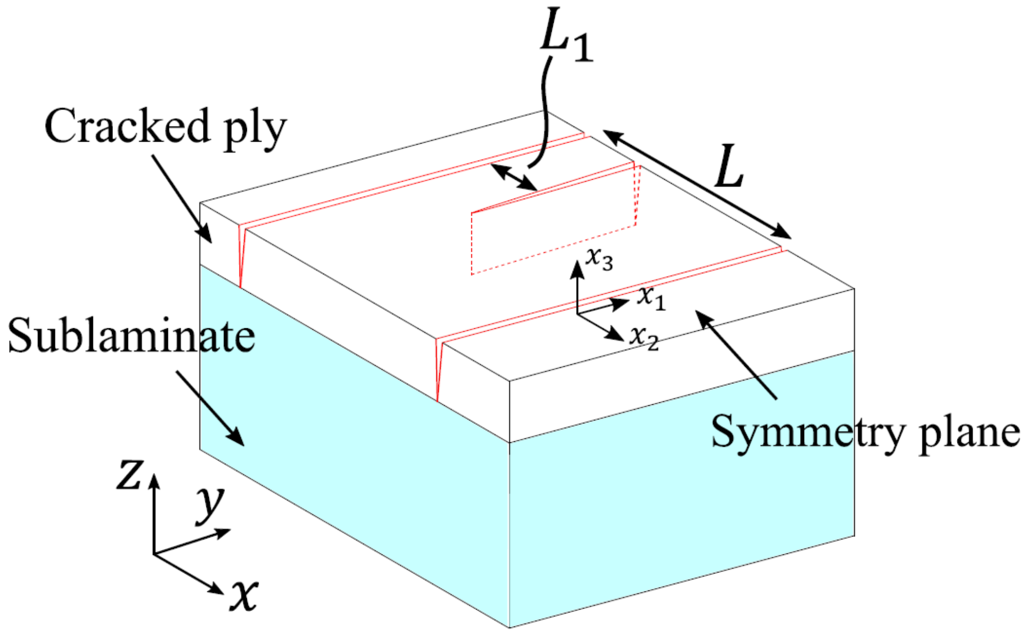

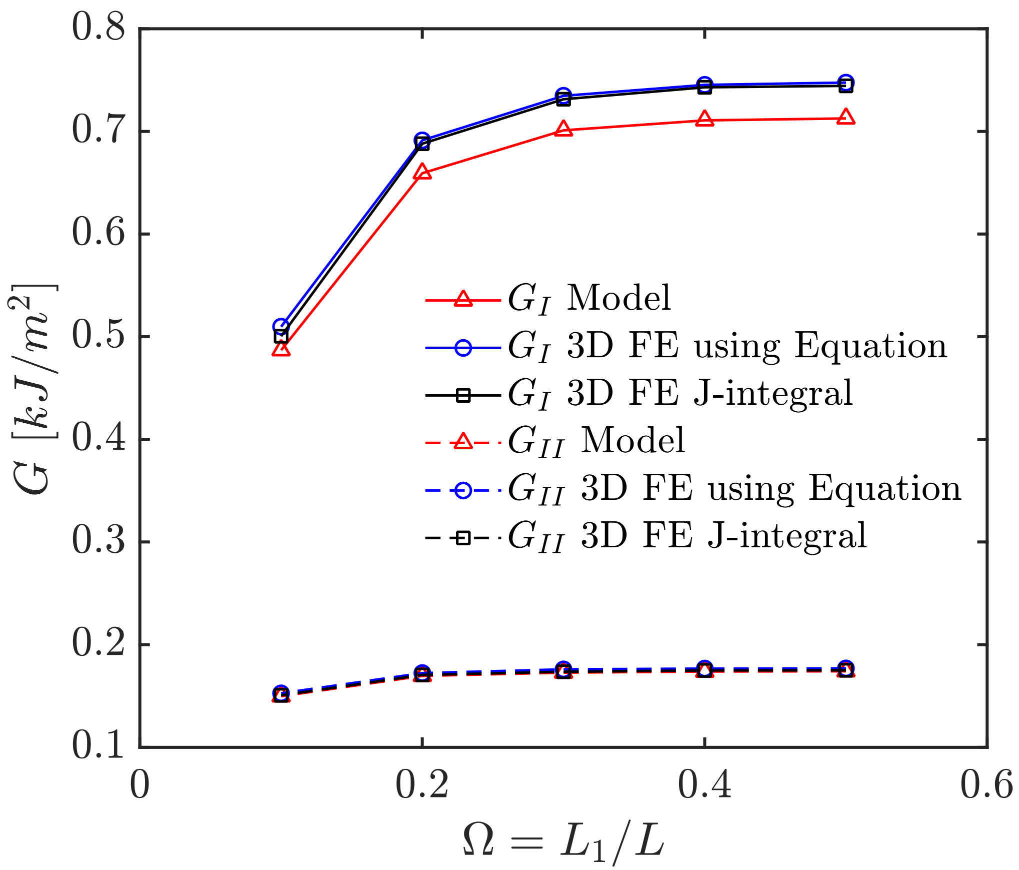

G_I and G_{II} in the thick 90° ply of $[0/90/0/\mathbf{-90}]_S$ under pure uniaxial and shear strains.

Growth of tunnelling cracks under strain-control

Tunnelling cracks in cruciform specimens

$\mathrm{BR} = \frac{\varepsilon_{yy}}{\varepsilon_{xx}}$	ε^p_{xx} $(\mu\varepsilon)$	ε^p_{yy} $(\mu\varepsilon)$
0.5	3000	1500

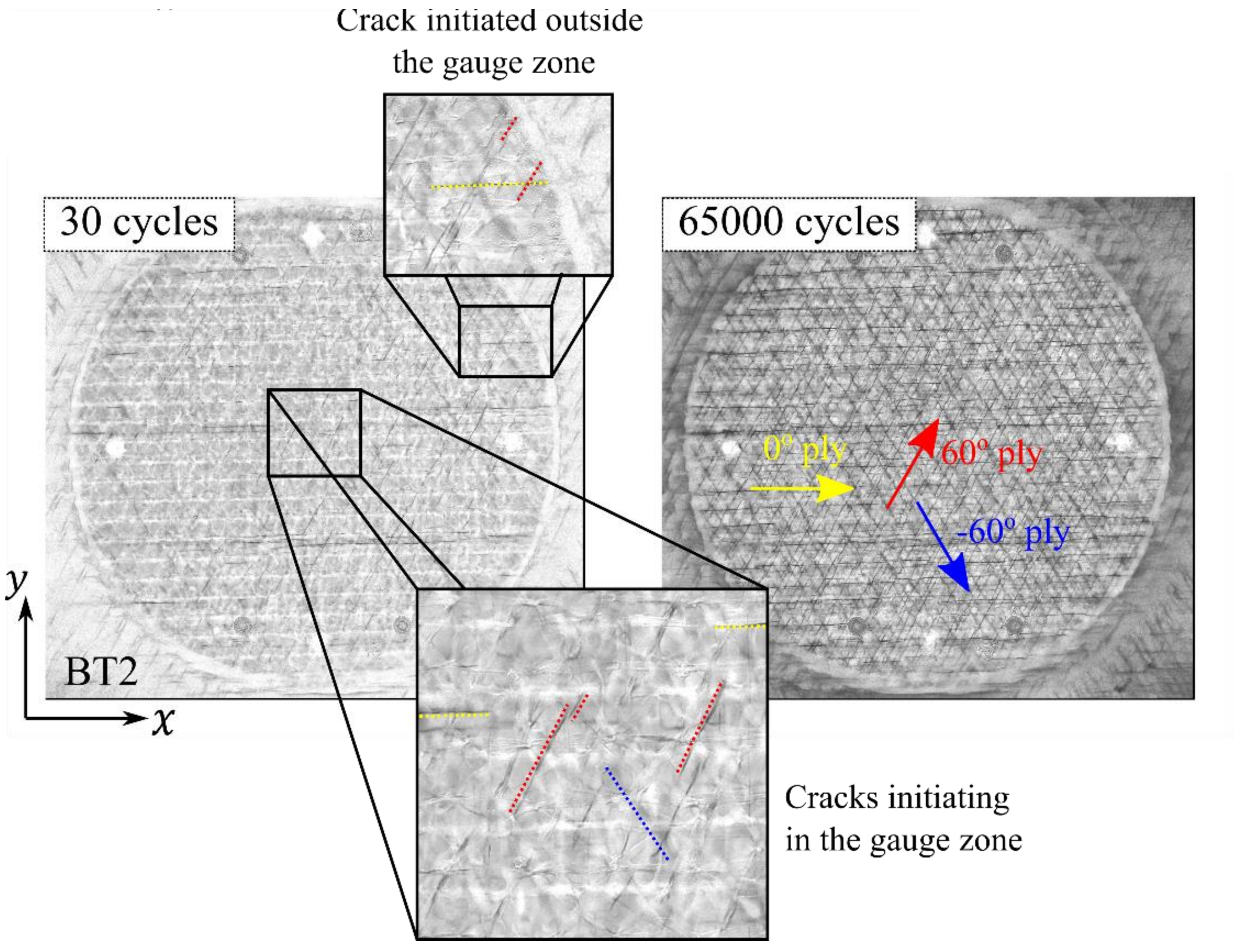

Growth of tunnelling cracks under strain-control

Tunnelling cracks in cruciform specimens

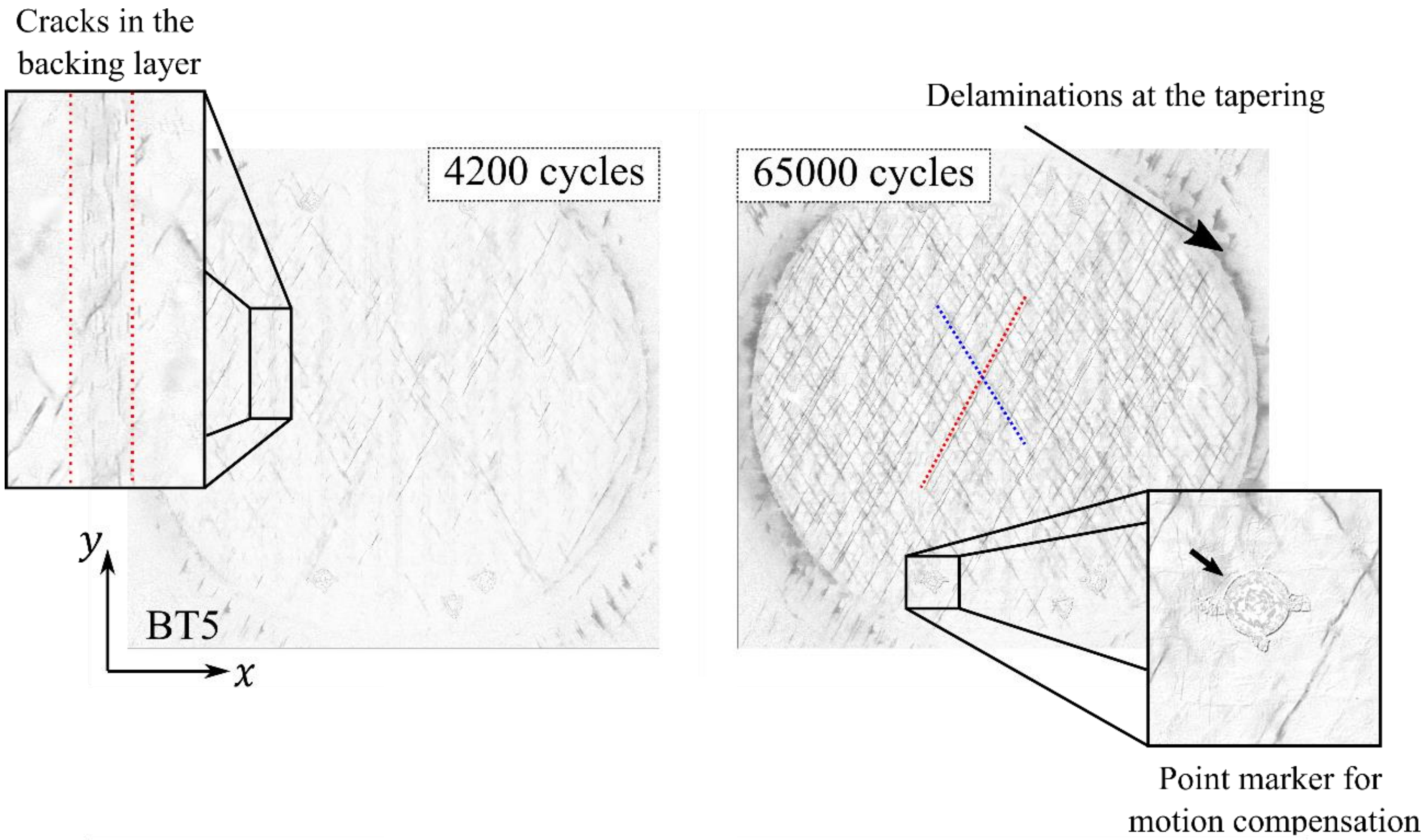

$BR = \frac{\varepsilon_{yy}}{\varepsilon_{xx}}$	ε_{xx}^{p} $(\mu\varepsilon)$	ε_{yy}^{p} $(\mu\varepsilon)$
-0.646	4000	-2584

4 Growth of tunnelling cracks under strain-control

Conclusions

- Cyclic tests at a single strain level can produce a Paris-Erdogan type of expression for crack front growth rate.
- Cycle tests at a single force level is still needed to characterize the variation associated with the crack front growth rate.
- Complicated cracking scenarios can potentially be reduced down to the simple cracking scenario where a crack is growing in between two bounding longer cracks.
- No effect of the crack front growth rate was found when collinear crack fronts are heading towards each other.
- The growth rate reduce only after non-collinear cracks cross-over each other.

5

Predicting crack density evolution

Predicting crack density evolution

Basic model framework

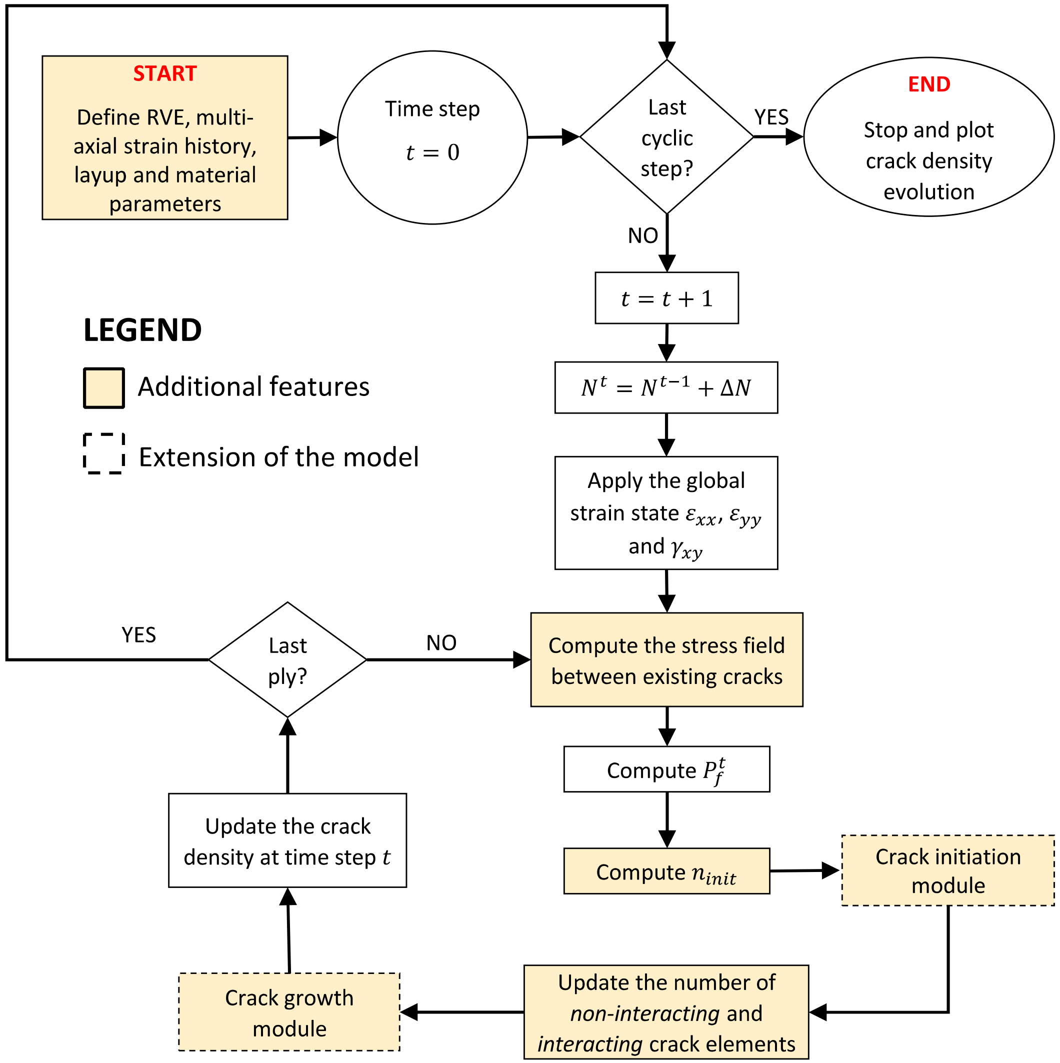

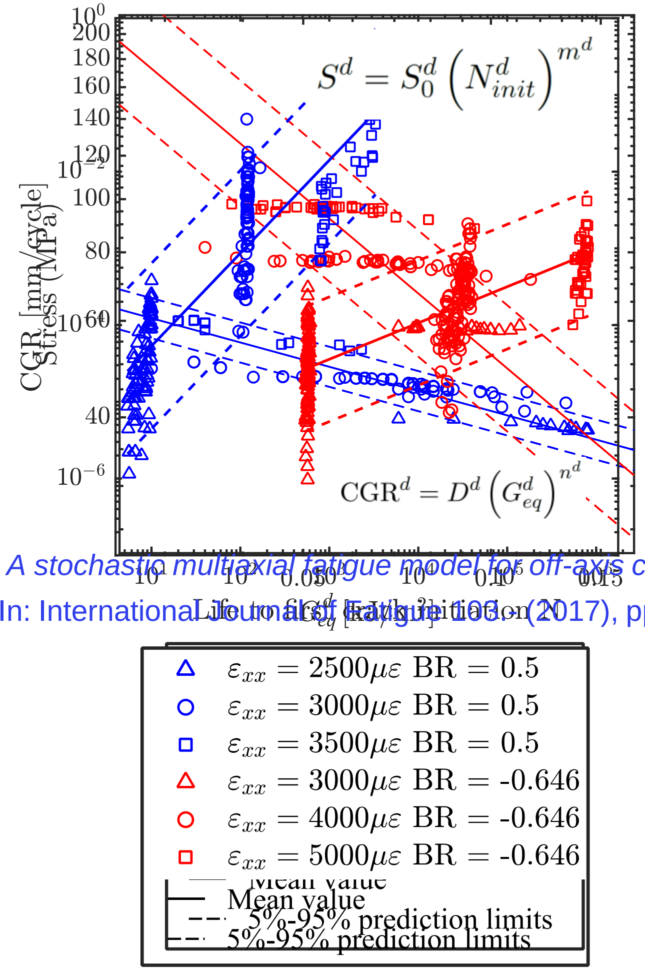

J.A. Glud et al. *A stochastic multiaxial fatigue model for off-axis cracking in FRP laminates*. In: International Journal of Fatigue 103 (2017), pp. 576–590

$$\mathrm{LHS} = \frac{\sigma_{rr} + \sigma_{\varphi\varphi} + \sigma_{zz}}{3}$$

$$\mathrm{LMPS} = \frac{1}{2}\left[\sigma_{rr} + \sigma_{zz} + \sqrt{\sigma_{rr}^2 + 4\sigma_{rz}^2 - 2\sigma_{rr}\sigma_{zz} + \sigma_{zz}^2}\right]$$

P.A. Carraro and M. Quaresimin. *A damage based model for crack initiation in unidirectional composites under multiaxial cyclic loading*. In: Composites Science and Technology 99 (2014), pp. 154–163

5 Predicting crack density evolution

Element discretisation

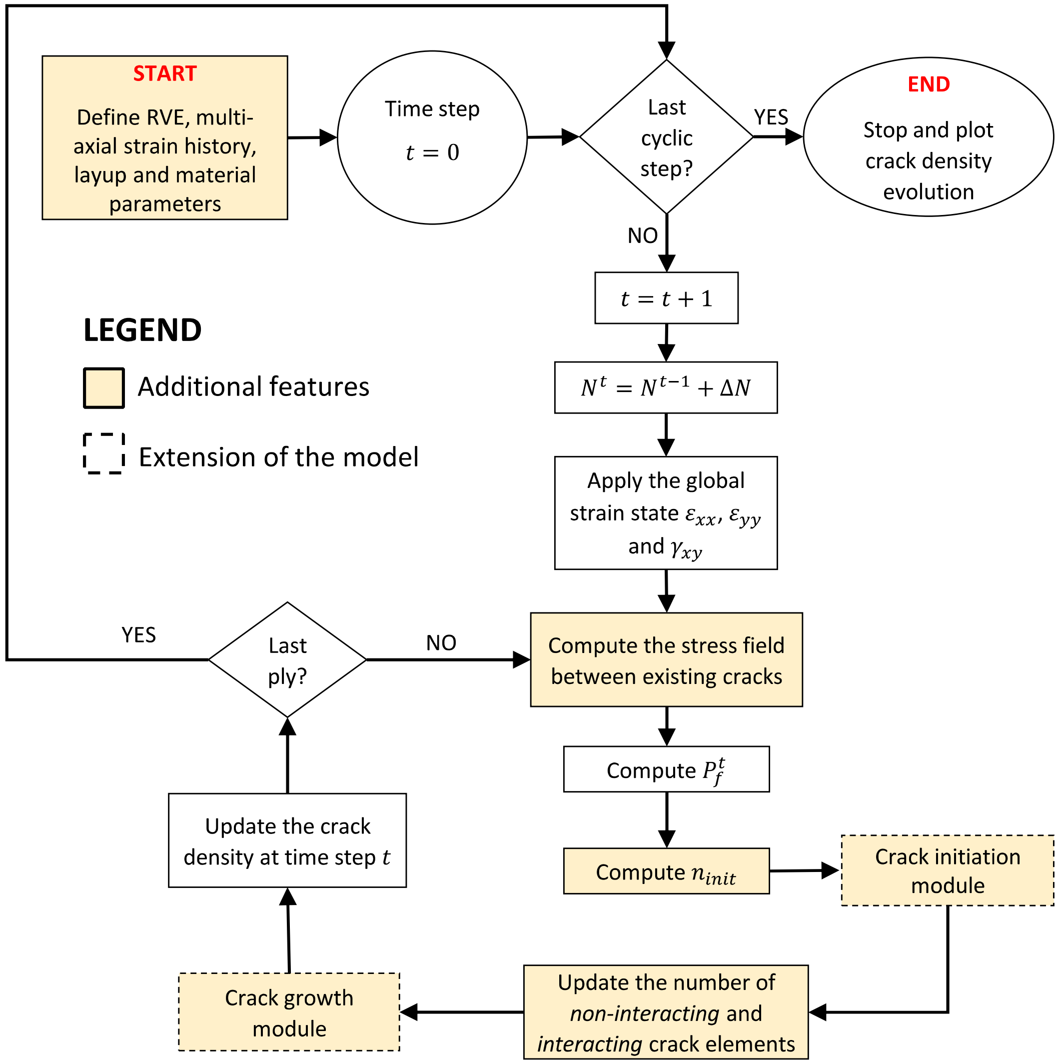

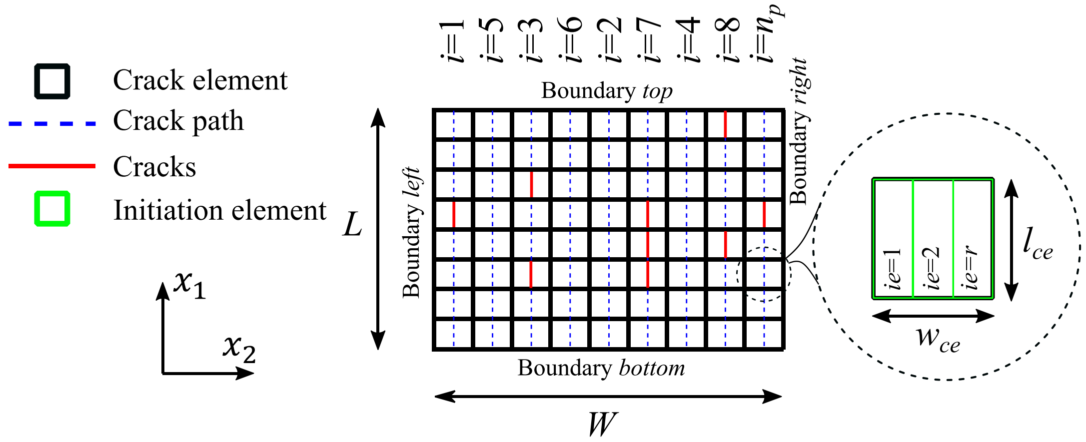

$$n_{ce} = \frac{L \times W}{l_{ce} \times w_{ce}} \qquad n_p = \frac{W}{w_{ce}} \qquad n_{ie} = r \times n_{ce}$$

$$\phi_p = n_{i,p}/L \qquad n_{init} = \left(\sum_{p=1}^{n_p} \phi_p L\right) P_f^t$$

$$P_f^t = 1 - \left(\prod_{ie=1}^{n_{ie}} P_s^{\mathrm{LHS}(ie)(t)}\right)\left(\prod_{ie=1}^{n_{ie}} P_s^{\mathrm{LMPS}(ie)(t)}\right)$$

J.A. Glud et al. *A stochastic multiaxial fatigue model for off-axis cracking in FRP laminates*. In: International Journal of Fatigue 103.- (2017), pp. 576–590

Predicting crack density evolution

Element discretisation

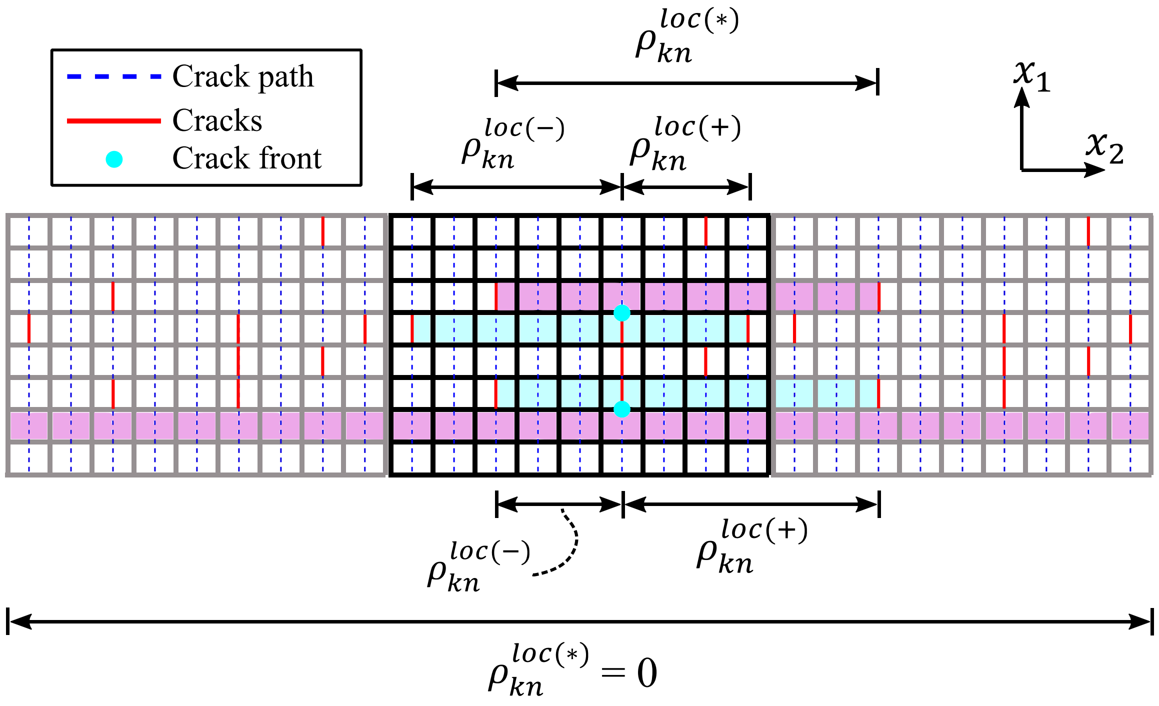

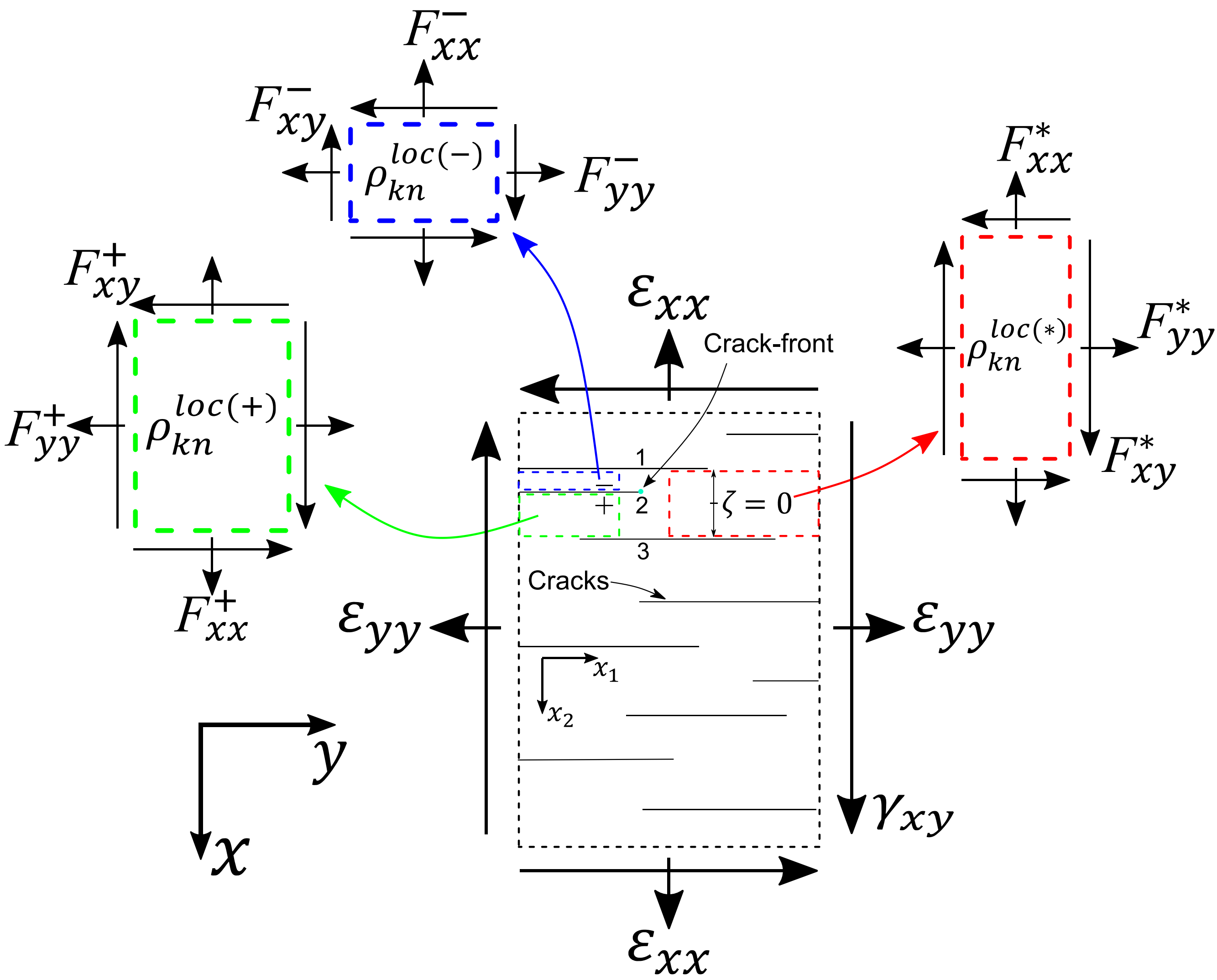

5 Predicting crack density evolution

Element discretisation

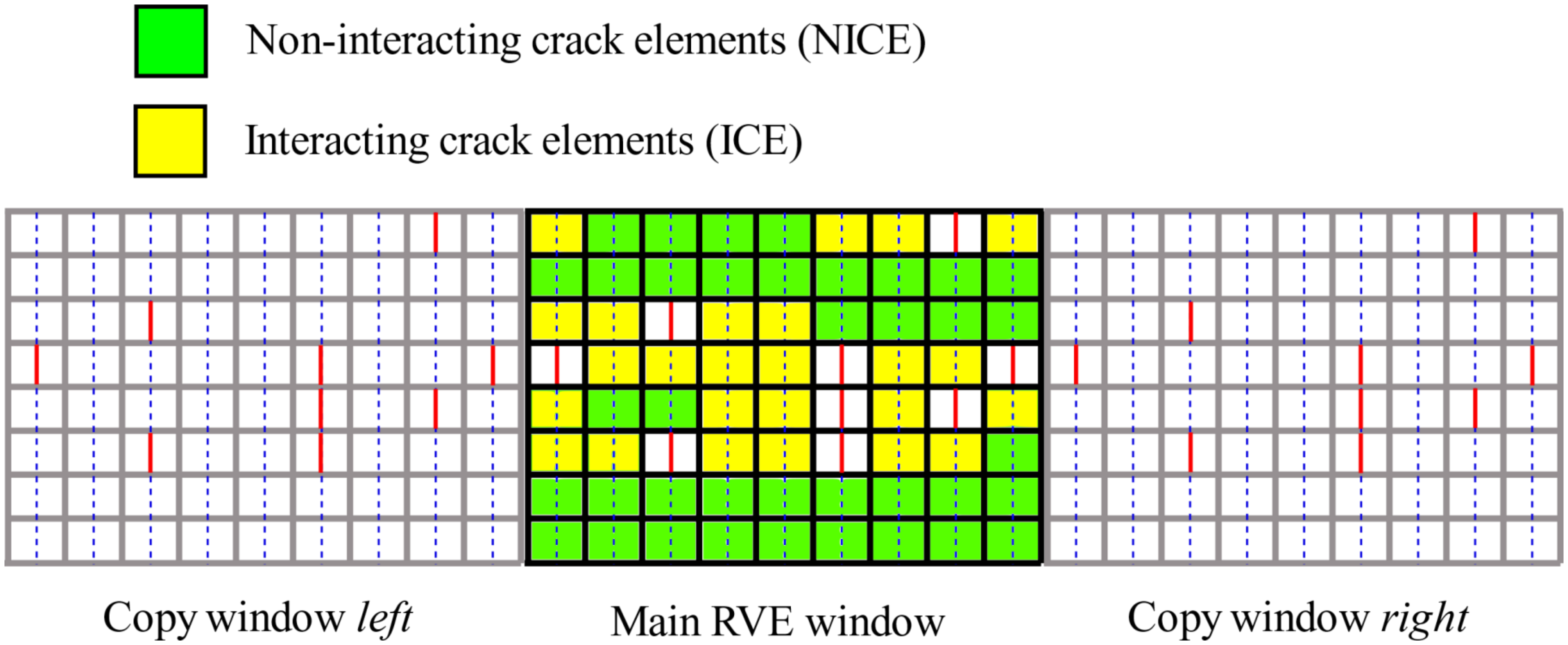

5 Predicting crack density evolution

Stochastics

CGR at a certain steady state ERR follows a Weibull distribution

$$P_c^d = 1 - exp\left(-\left[\frac{\text{CGR}^d}{D^d\left(G_{eq}^d\right)^{n^d}}\right]^{\beta_c^d}\right)$$

Life to crack initiation for the LHS and LMPS damage modes follows a Weibull distribution under a constant stress level

$$P_f^d = 1 - P_s^d = 1 - exp\left(-\left[\frac{N_{init}^d}{\left(\frac{S^d}{S_0^d}\right)^{1/m^d}}\right]^{\beta_s^d}\right)$$

J.A. Glud et al. *A stochastic multiaxial fatigue model for off-axis cracking in FRP laminates*. In: International Journal of Fatigue 103.- (2017), pp. 576–590

Predicting crack density evolution
Crack initiation module

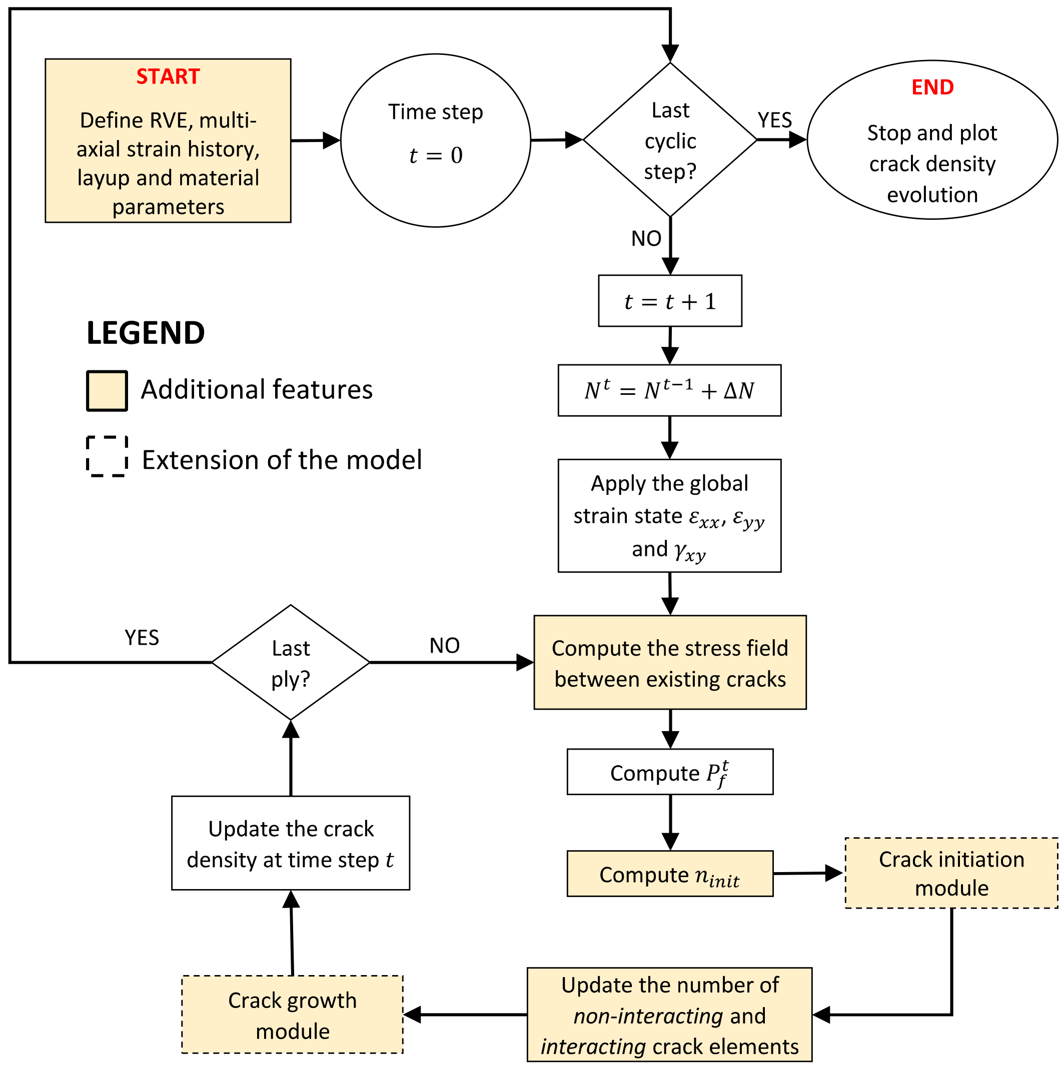

Initiation of cracks depend on various factors –

- Stress state in the ply
- Local micro-structure
- Defects, etc.

The total probability of failure of the laminate also does not provide the location of the cracks explicitly.

Predicting crack density evolution

Crack initiation module

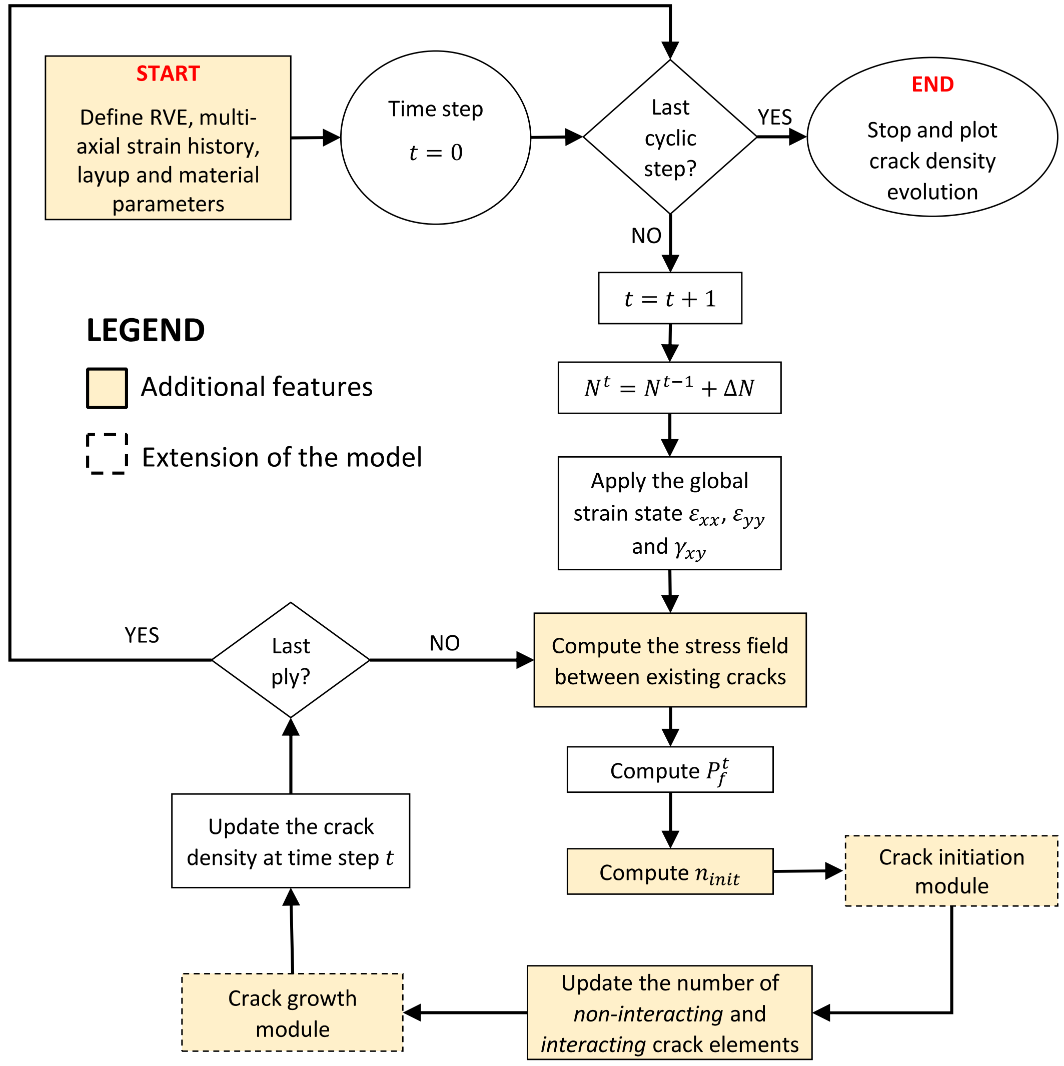

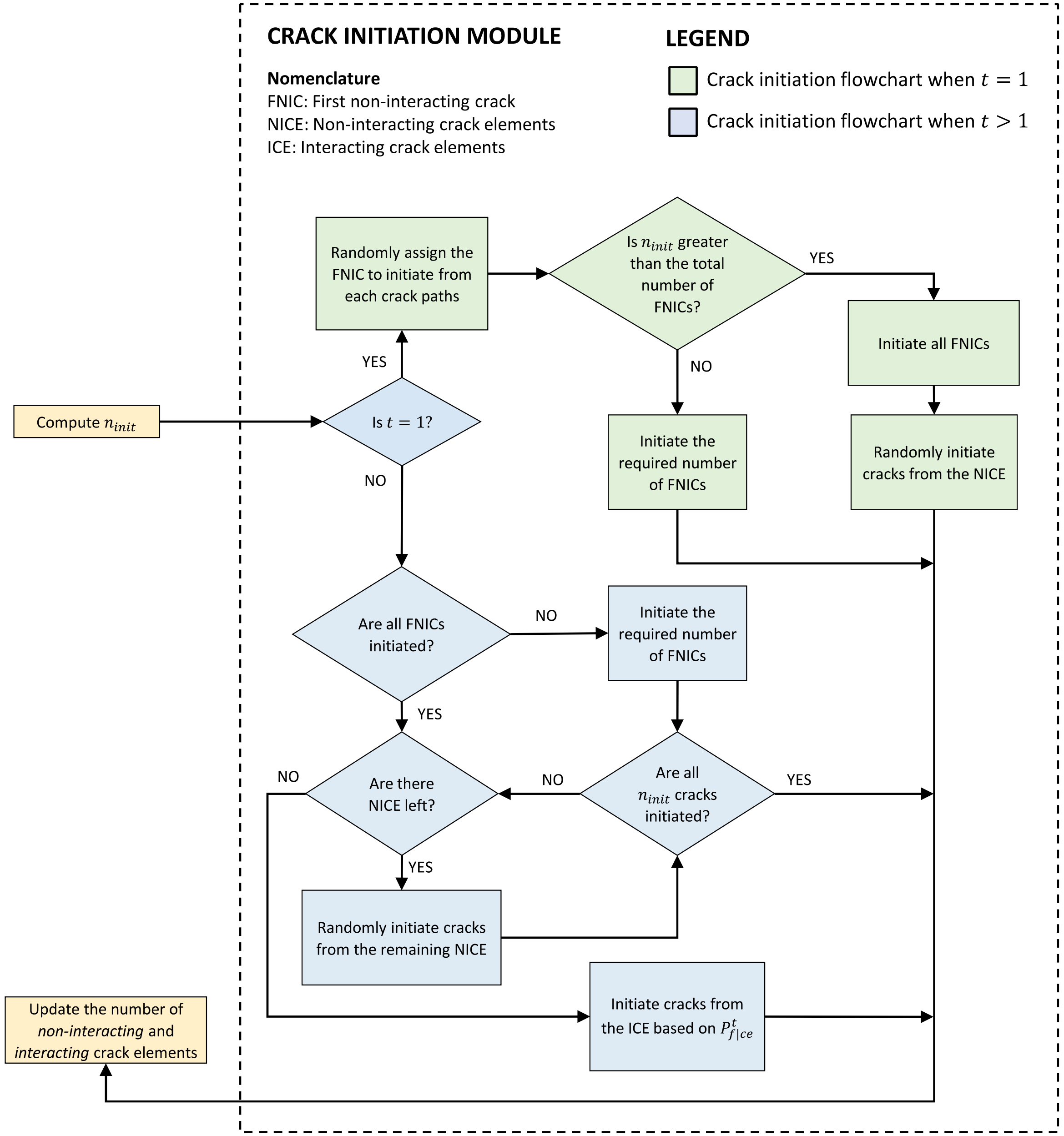

5 Predicting crack density evolution

Crack growth module

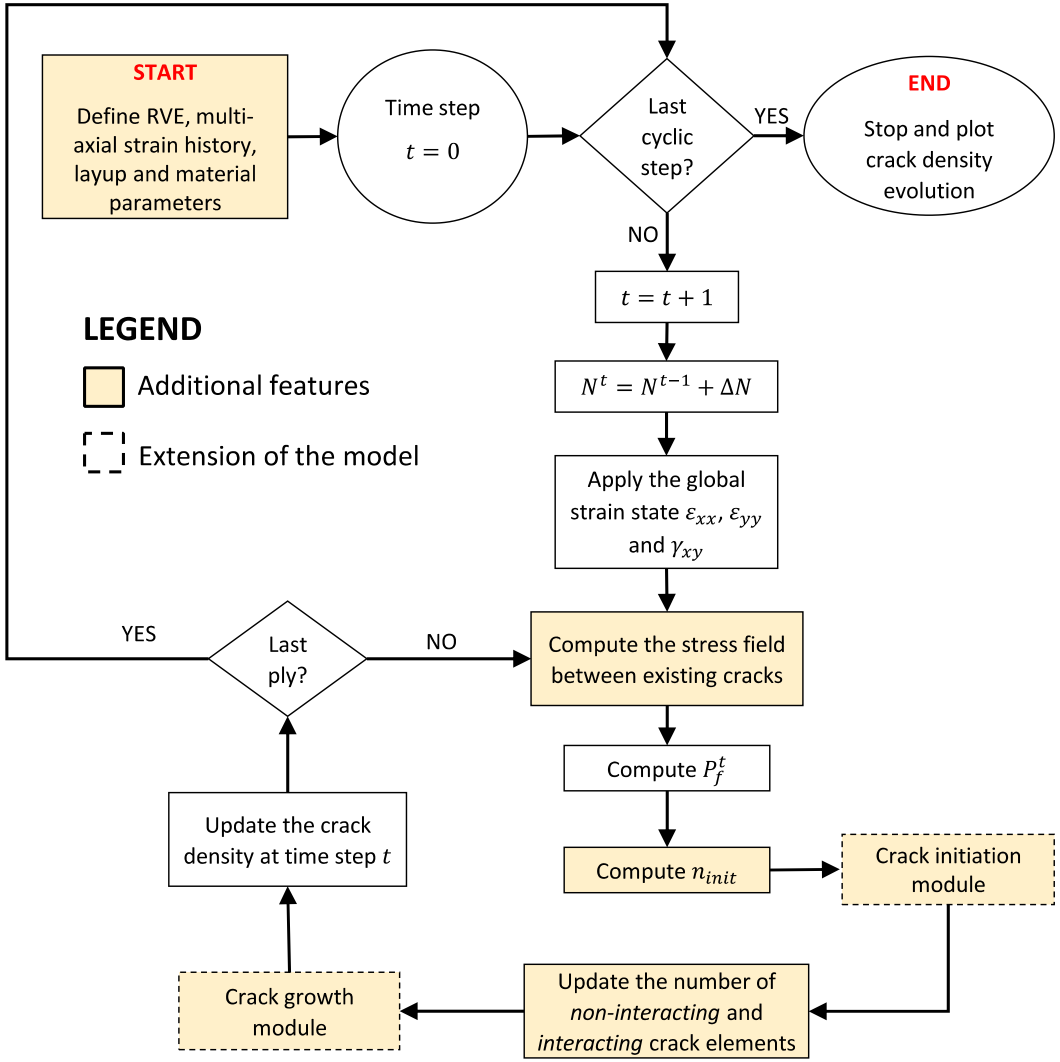

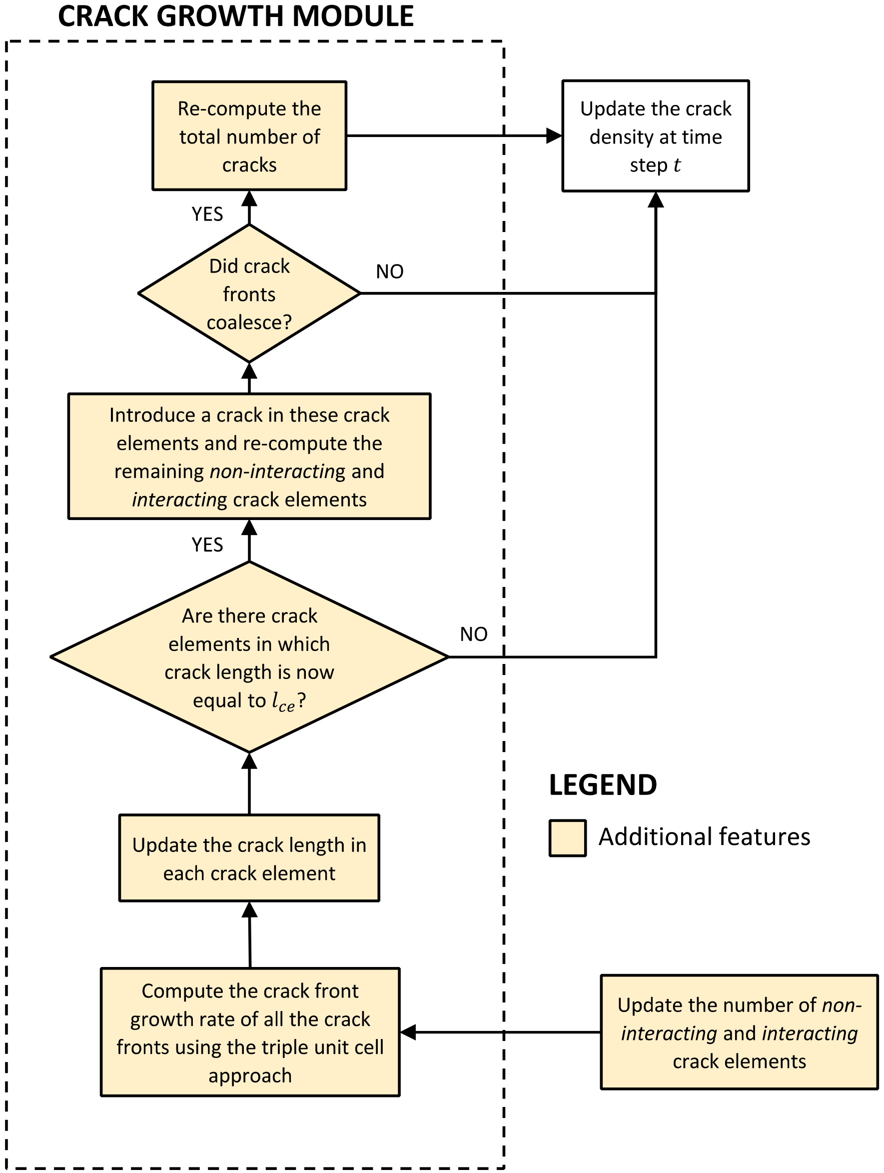

5 Predicting crack density evolution

Results

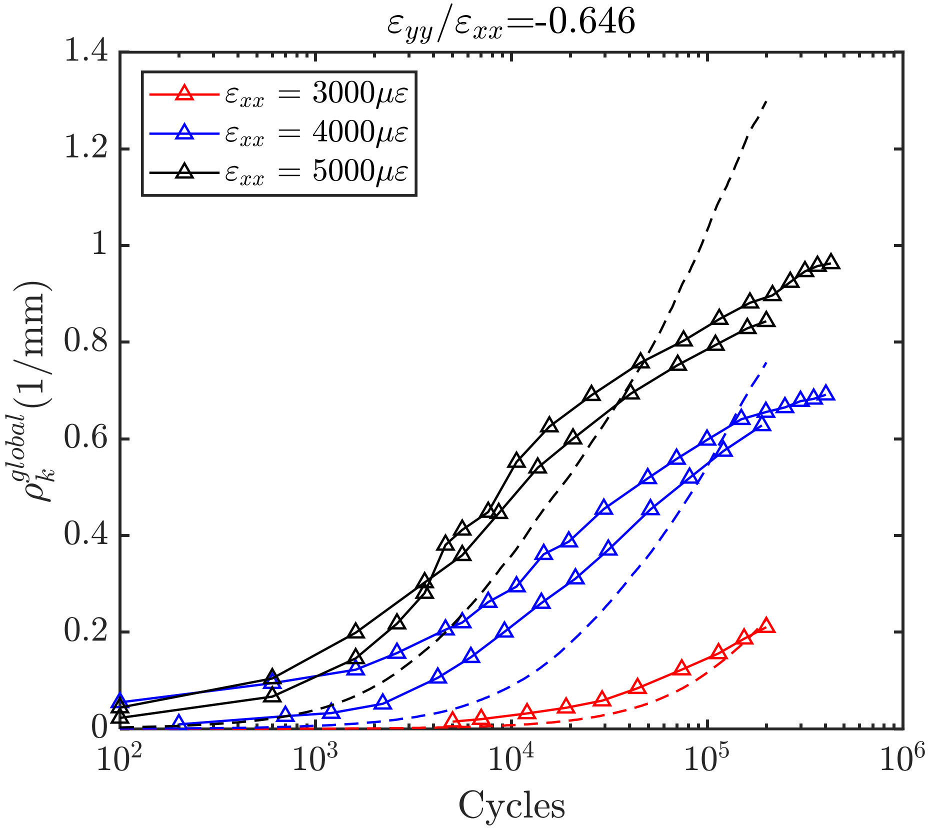

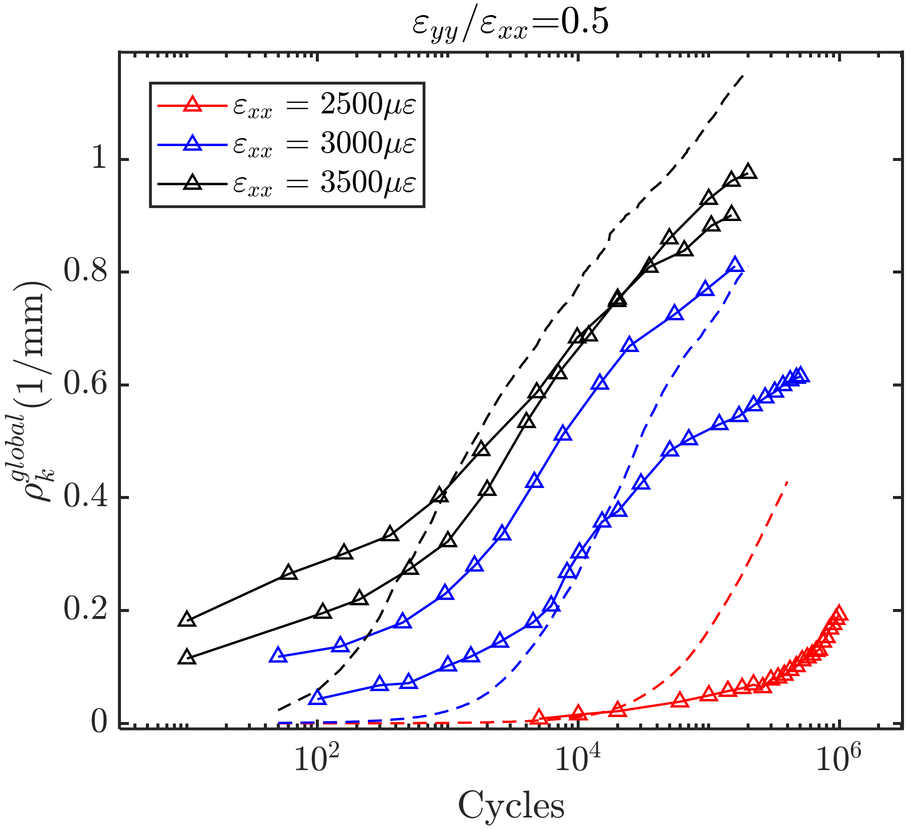

60° ply of $[0/60/0/-60]_S$

Predicting crack density evolution
Results

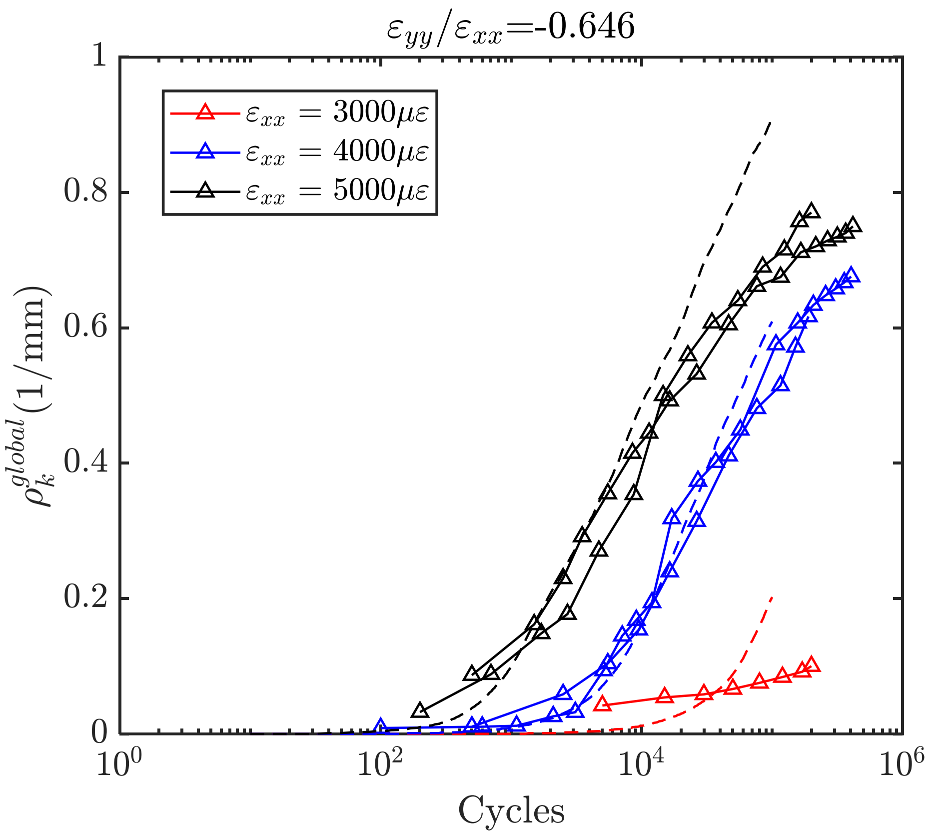

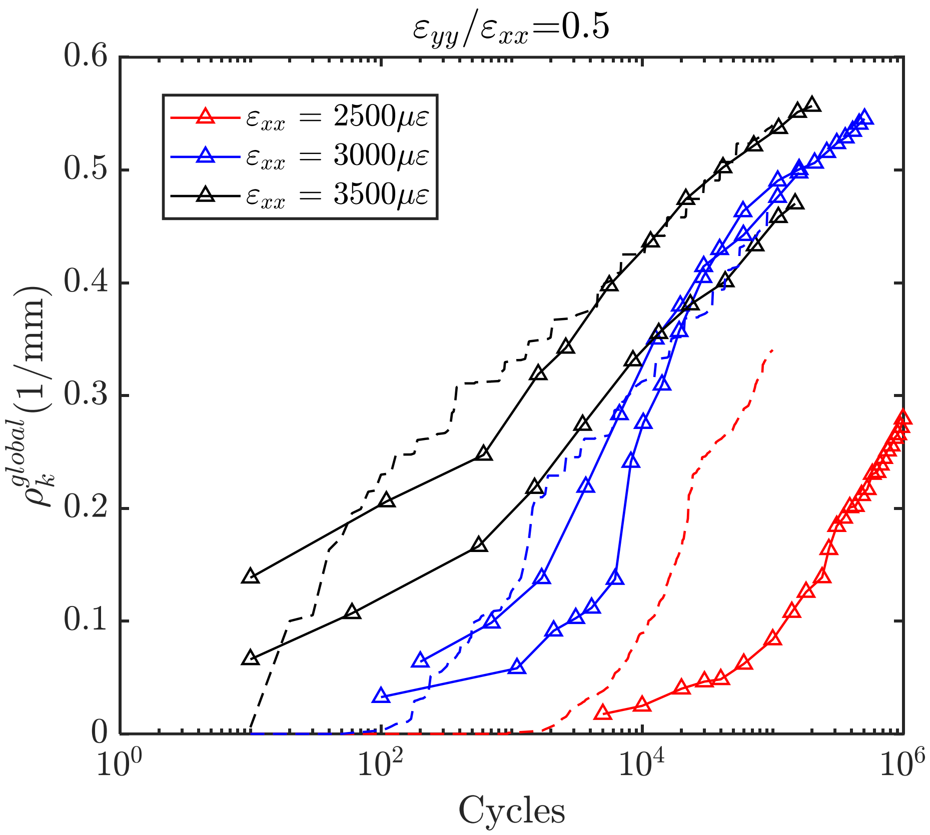

-60° ply of $[0/60/0/-60]_S$

5 Predicting crack density evolution

Results

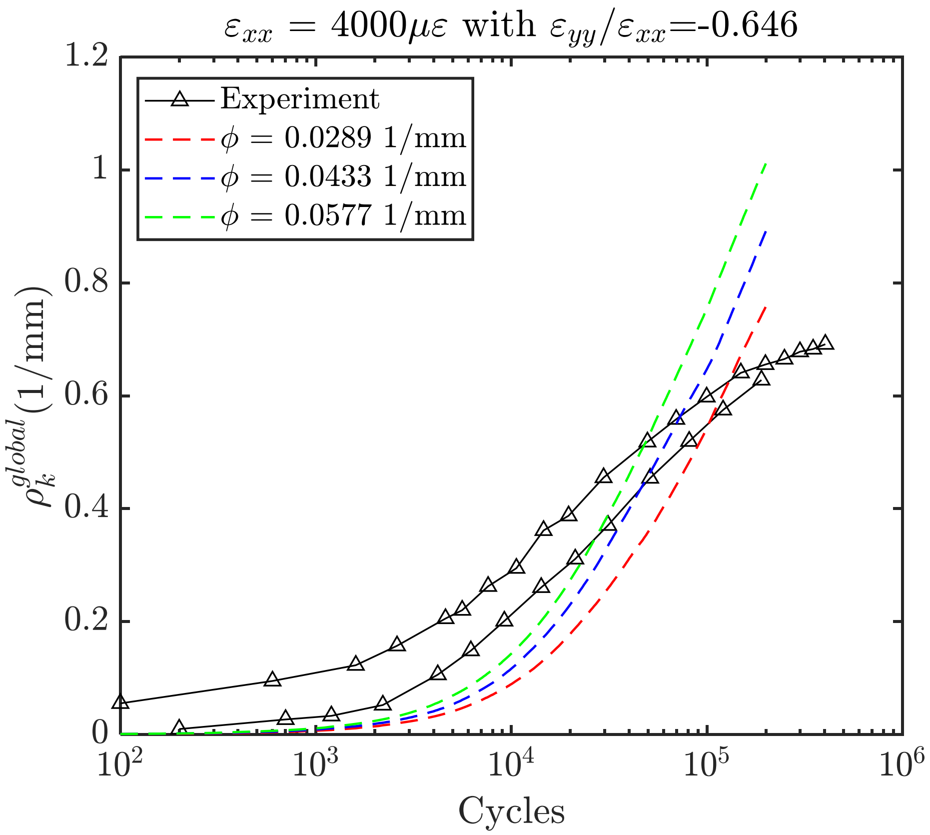

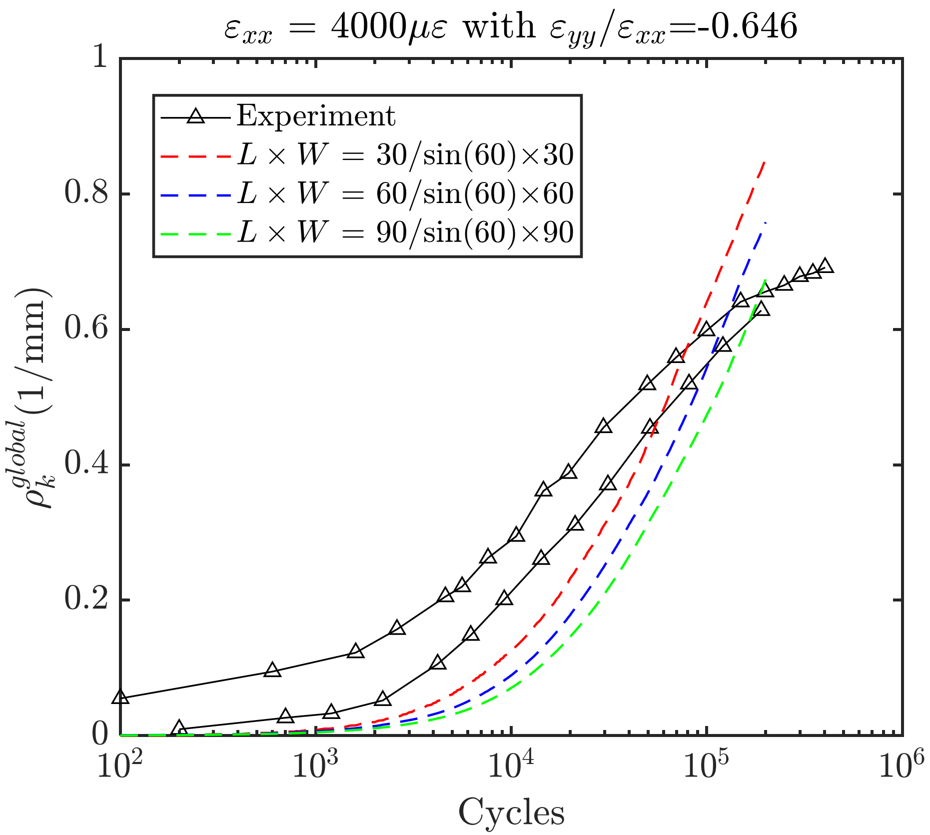

60° ply of $[0/60/0/-60]_S$

5 Predicting crack density evolution

Conclusions

- The model allows for crack initiation anywhere in the laminate as well crack coalescence.
- The ERR of crack fronts are explicitly calculated based on the local cracking conditions around the crack front.
- Cruciform specimens are used for calibrating the damage model to avoid using equivalent uniaxial laminates.
- The model predictions was found to be conservative at high crack density for the thin layer, but presented fairly good predictions for the thick layer.
- The model prediction was found to be heavily influence by the choice of parameter ϕ_p.
- The model accounts for the growth of damage outside the primary RVE, but as of now does not account for cracks entering into the main RVE from outside.

6

The future for cruciform specimens

6 The future for cruciform specimens

Comparison with PhD1 and PhD3

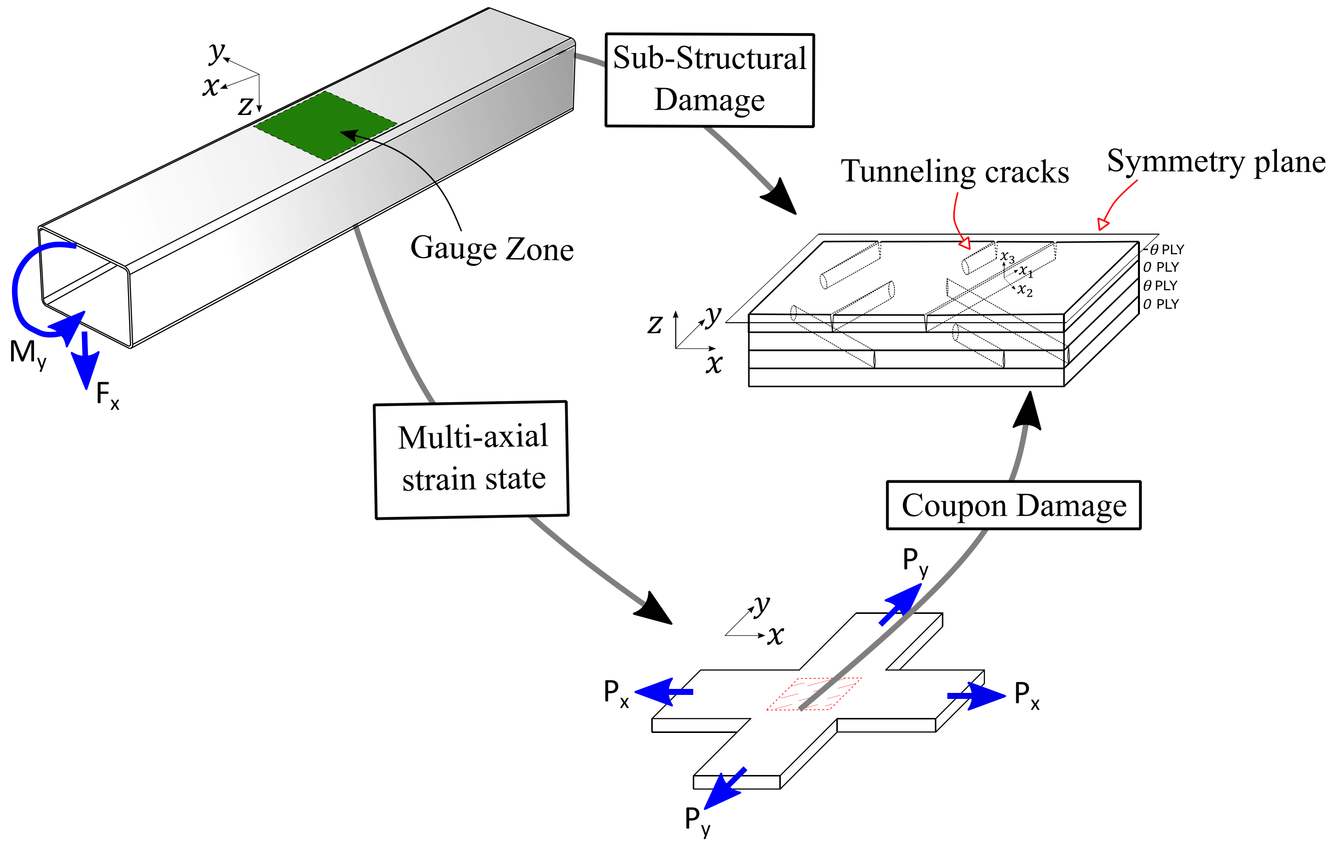

Comparison of the **global crack density evolution**, such that the biaxial strain states of the two gauge zones are similar.

The future for cruciform specimens
Comparison with PhD1 and PhD3

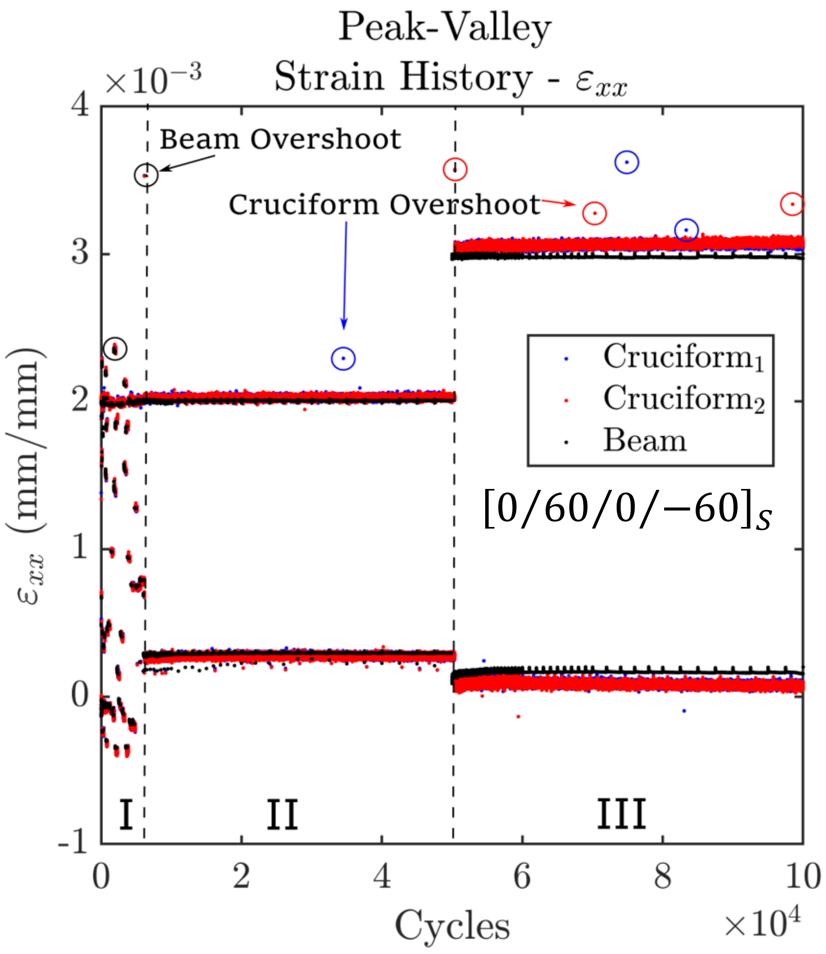

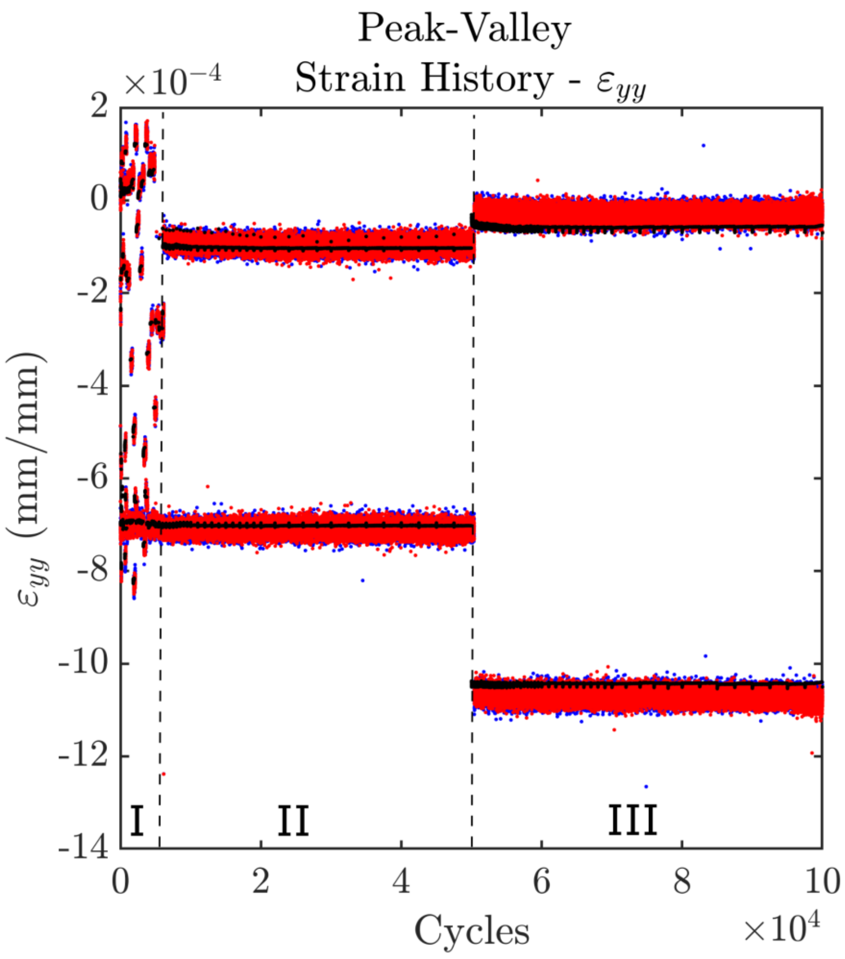

The future for cruciform specimens

Comparison with PhD1 and PhD3

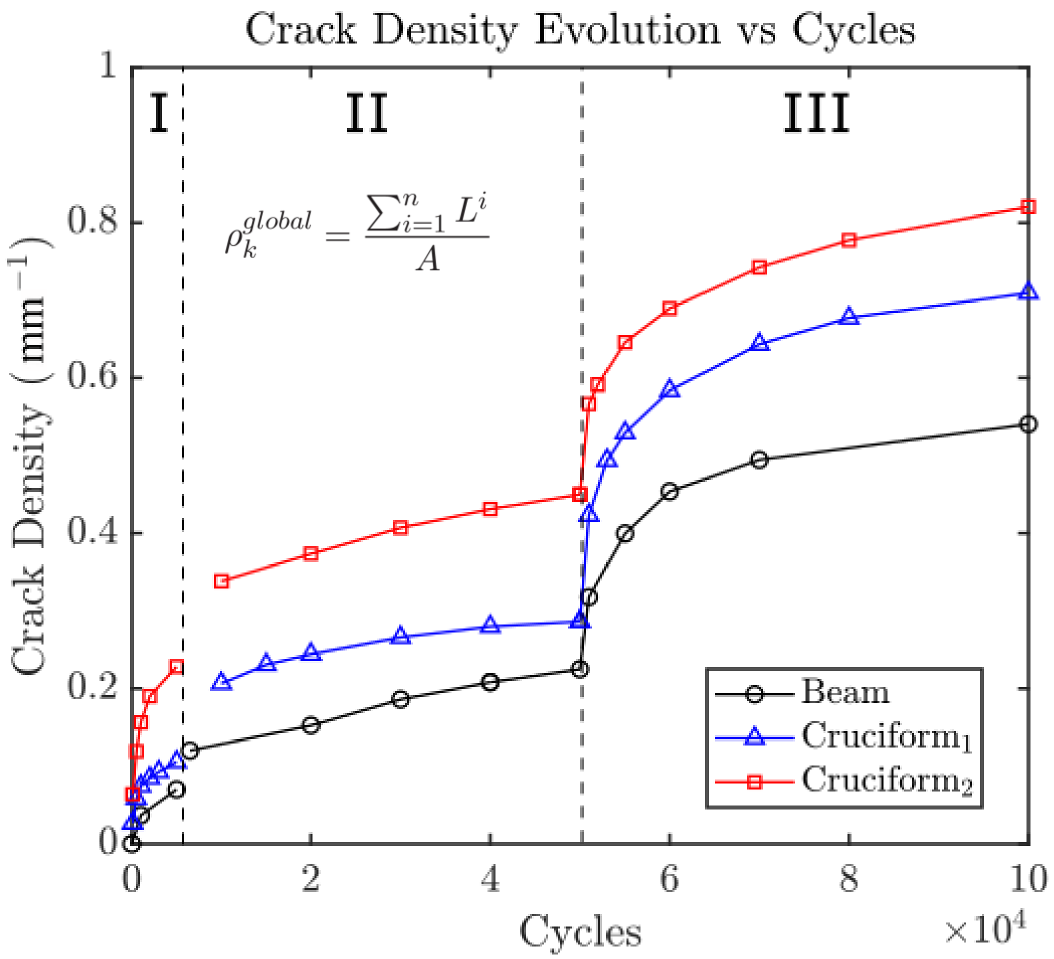

The future for cruciform specimens

Comparison with PhD1 and PhD3

Comparison of the growth of **non-interacting** tunnelling cracks from within the gauge zone of the cruciform specimen and an **equivalent** uniaxial specimen.

That is, the average **energy release rate** and the **mode-mixity** of the crack fronts from the equivalent uniaxial specimen was similar to the cracks fronts from the cruciform specimen.

The **specimen layup** and the **load magnitude** of the equivalent uniaxial specimen are altered.

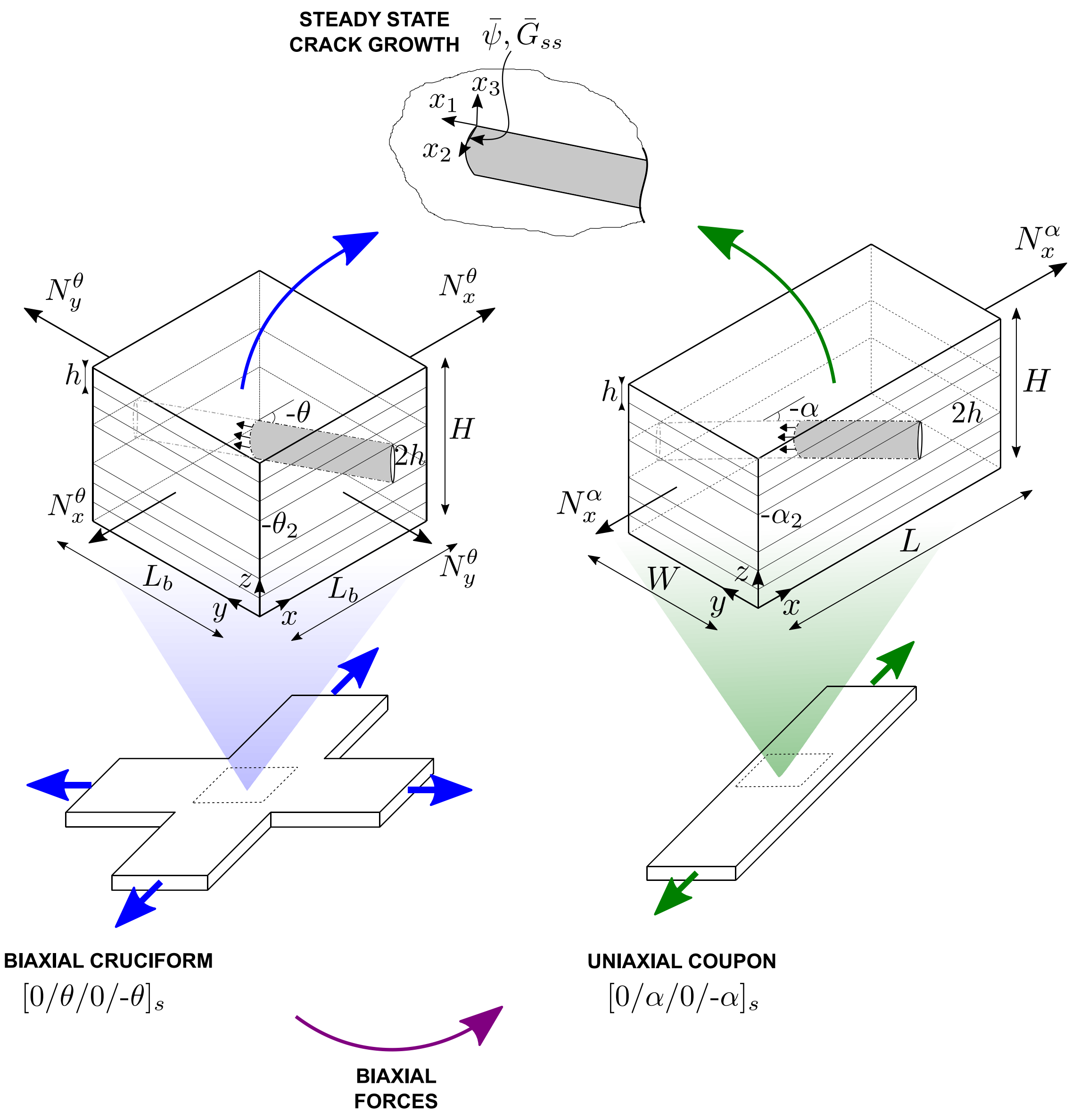

A.K. Bangaru et al. *Approach for analysing off-axis tunnelling cracks in biaxially loaded laminates*. In: Composite Structures 269 (2021), p. 113935

6 The future for cruciform specimens

Comparison with PhD1 and PhD3

6 The future for cruciform specimens

Conclusions

- The strain state from a sub-structural beam specimen was successfully recreated in the gauge zone of the cruciform specimen.
- The crack density evolution was found to be higher than the beam specimen.
- The stochastic nature associated with crack density evolution was not captured here.
- The crack front growth rate of non-interacting crack fronts in cruciform specimens were lower than the growth rate observed in the uniaxial specimen.
- Reproducing damage in different length scales is not a trivial task.
- Attention needs to be paid to design of specimen as recreation of the biaxial strain state even though is a necessary condition, but not a sufficient condition.
- Specimens should share identical boundary conditions.

Presentation is based on the following journal publications

- **A. Moncy**, O. Castro, C. Berggreen, H. Stang*, Understanding the effect of anisotropy in composite materials on the performance of cruciform specimens*, Composite Structures (2021)

- **A. Moncy,** J. Waldbjørn, C. Berggreen, *Biaxial strain control fatigue testing strategies for composite materials*, Experimental Mechanics (2021)

- **A. Moncy,** B.F. Sørensen, O. Castro, C. Berggreen, J.A. Glud, *Propagation of tunnelling cracks in composite materials under strain and force-controlled cyclic loading*, Journal of Composite Materials (2022)

- **A. Moncy**, O. Castro, J.A. Glud, C. Berggreen, O.T. Thomsen, J.M. Dulieu-Barton, *A tunnelling crack density evolution model for FRP laminates subjected to cyclic multi-axial strain-controlled loading*, (under review - 2023).

- A. Quinlan, **A. Moncy**, A. Bangaru, O. Castro, H. Stang, C. Berggreen, L.P. Mikkelsen, A. Michel, B.F. Sørensen, *Multi-scale experimental analysis of tunneling cracks in composite laminates under cyclic loading*, (In Manuscript/Preparation - 2023).

DTU

Thank you for your attention